Evaluating biochar and fungi for the remediation of PFAS in landfill leachates

Rushirajsinh Chauhan

A thesis submitted in fulfillment of the requirements

for the degree of Master of Engineering

Main supervisor: Graeme Glasgow

Co-supervisor: Mark Lay

School of Engineering

The University of Waikato

New Zealand

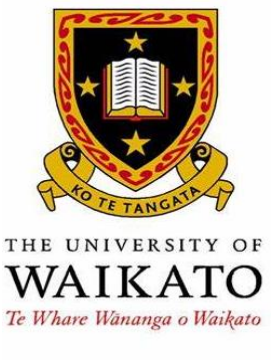

2024

Abstract

Per- and polyfluoroalkyl substances (PFAS) have become widespread environmental contaminants, often detected in various ecosystems, including waterways, and found in numerous products such as cosmetics. In New Zealand, PFAS contamination poses a significant risk to both environmental and human health. This study works towards developing an innovative PFAS removal technology utilizing biochar to adsorb PFAS and fungi to degrade PFAS. The work was broken into several stages, the first finding suitable growing conditions for fungi on biochar and attempting to quantify the growth, the second examining biochar adsorption properties, first with humic acid and the second with PFAS. Three different types of fungi, Oyster, Shiitake, and Pekepeke (native to New Zealand), were cultivated on biochar and substrates made from woodchips and other organic materials. Growth was best on a combination of biochar and woodchip. The chloroform fumigation method showed that the oyster/biochar culture had a growth of 17.6 mg/g/day, while shitake/biochar was 14.6 mg/g/day and the oyster/biochar/woodchip had a growth of 20.7 mg/g/day.

Biochar had a low adsorption capacity (5 mg/g) and affinity for humic acid. The Freundlich isotherm gave a marginally better fit to adsorption data than the Langmuir and SIPS isotherms. The low adsorption was due to both humic acid and biochar having predominantly negative charges, biochar had a surface charge of 0.824 mM -ve charges/g biochar, six times that of dry soil which has a surface charge of 0.125 mM/g soil. Biochar was tested for its ability to adsorb three species of PFAS (PFBSA, PFHexA, PHHepA). Under the environmentally relevant PFAS concentration ranges tested, biochar adsorbed all of the PFAS, resulting in no PFAS being able to be detected in solution. PFAS adsorption to the biochar is predominantly by hydrogen bonding.

Preface

This thesis is submitted to the University of Waikato, New Zealand, in partial fulfilment of the requirements for a master's degree in environmental engineering. The work presented here has not been submitted for any degree or diploma at any other institution. To the best of my knowledge, this thesis contains no material previously published or written by others, except where proper citation is provided.

Acknowledgments

First and foremost, I would like to express my deepest gratitude to my main supervisor, Graeme Glasgow, and my co-supervisors, Mark Lay, and my Lab assistant Steven Wu for their unwavering support throughout my research journey. Their guidance and invaluable contributions were instrumental in the successful completion of my thesis, and they have greatly shaped my growth as an independent researcher.

I am particularly grateful to Steven Wu for his insightful feedback and assistance with the experiment's challenges, which were crucial throughout the process. I also extend my heartfelt thanks to Graeme Glasgow for his constant encouragement and support, which played a significant role in my progress.

I deeply appreciate the support from Bhavyarajsinh Kher, Neel Patel and Yash Lakhani whose encouragement has been a cornerstone during this journey. I also sincerely appreciate my well-wishers in New Zealand, whose encouragement has been vital in shaping this thesis.

My deepest gratitude goes to my mother, father, sister, and uncle Mr.K.P Raju for their unwavering support throughout the year. I also want to thank my whole family and friends in India, whose love and encouragement have been a constant source of strength.

Lastly, special thanks to the University of Waikato, School of Engineering, for providing the necessary computing resources and research assistance.

Notation

Per- and poly-fluoroalkyl substances	PFAS
Perfluorobutanesulfonic acid	PFBSA
Perfluorohexanoic acid	PFHexA
Perfluoroheptanoic acid	PFHEPA
Organization for Economic Co-operation and Development	OECD
perfluoro octane sulfonates	FOSA
fluorotelomer alcohols	FTOH
Perfluorooctanesulfonic acid	PFOS
Perfluorononanoic acid	PFNA
perfluoroalkyl acids	PFAA
perfluorooctanoic acid	PFOA
Nano gram per liter	ng/L
Micrometer	μm
granular activated carbon	GAC
Mili Q water	DI water
Adsorption	ADS
Miligram per liter	mg/L
Milligram per gram	mg/g
Grams per liter	g/L
Grams per mole	g/mol
Limit of Quantification	LOQ
Surface charge	mV

Contents

List of Figures

List of Tables

Chapter 1- Introduction

1.1 Background

Per- and poly-fluoroalkyl substances (PFAS) are chemical compounds that have multiple fluorine groups attached to an alkyl chain. They are used to make fluoropolymer coatings that resist water, oil, and heat for clothing, furniture, food packaging, cooking appliances, as well as in cosmetic products, and firefighting foams. They are difficult to degrade with half-lives of over eight years, mobile in soil and water, and bioaccumulate in the food chain. PFAS has been detected in groundwater at over 2000 different locations in the United States, predominantly at Department of Defense fire-training facilities (Meegoda Jay N., 2022). In New Zealand, PFAS has been detected in 47% of groundwater wells. In particular, investigations at the Royal New Zealand Air Force base in Woodbourne and New Zealand Defence Force base in Devonport showed a contaminated water with PFAS in concentrations up to 78,000 ng/L and in a plume extending up to seven kilometers from the Woodbourne site (Laura, 2023). Exposure to PFAS has been linked to cancers, thyroid disease, decreased immunity, decreased fertility, reduced infant and fetal growth and developmental issues in children. Conventional wastewater treatment will not remove PFAS from raw wastewater sources such as wastewater treatment plants and landfill leachates.

PFAS will readily adsorb to biochar and activated carbon with some researchers reporting adsorption capacities of 40-80 mg PFAS per gram biochar , however this results in a compound heavily contaminated with PFAS that must then be disposed of or treated. Treatment methods include electrochemical oxidation (71-99.7% removal), (Zang yinjie, 2023) incineration e.g. using plasma (90->99% removal), and other oxidation techniques (99% removal). While these are effective, they have high energy consumption, high material consumption, forms toxic side products, or results in toxic emissions (Meegoda Jay N., 2022)

Bioremediation is another option for treatment of PFAS where certain bacterial strains of *pseudomonas, acidimicrobium* and *gordonia* will remove between 32 to 75% of the PFAS over periods from 2-100 days (Shahsavari Esmaeil, 2021). Research examining mycoremediation of PFAS using fungi is limited to wood-rotting fungus *Phanerochaete chrysosporium* where it removed 50% of 2-(Perfluorohexyl)ethanol (6:2 FTOH) within 28 days. While bioremediation is extremely slow compared to electrochemical oxidation, plasma, incineration and other oxidation techniques, it could be used in conjunction with biochar to immobilize the PFAS to give fungi or bacteria time to degrade the PFAS, and overall would be less expensive than the oxidation or thermal techniques.

This thesis presents research involved in working towards developing a coupled system for PFAS treatment which involves using biochar for rapid capture and fungi populating the biochar to degrade the PFAS. The work was broken into several stages, the first finding suitable growing conditions for fungi on biochar and attempting to quantify the growth, the second examining biochar adsorption properties with humic acid and PFAS.

Chapter 2- Literature Review

2.1 Overview

This thesis focuses on PFAS and various removal technologies, particularly through the use of biochar and other materials. It examines the impact of PFAS on human health, its presence in waterways, soil, and plants, and provides a detailed analysis of biochar's properties and applications. The study also covers adsorption as a key mechanism for PFAS removal, highlighting the role of adsorbents. Furthermore, it discusses landfill leachate treatment methods and concludes by addressing the current state of PFAS contamination in the environment, with a specific emphasis on the measures being taken in New Zealand to mitigate its effects.

2.2 Per- and poly-fluoroalkyl substances (PFAS)

Establishing a universal definition for PFAS is challenging because it is constantly changing based on its applications. PFAS, or poly and perfluoroalkyl substances, are man-made chemicals used in various industries since the 1940s. They were originally used in products like Teflon® and Scotchgard™, but are now found in food packaging, cosmetics, waterproof textiles, and firefighting foams (Sinclair Georgia M., 2020)

Originally, PFAS were regarded as non-toxic and inert, leading to little consideration of their potential impact on human and ecological health or their environmental persistence. However, in recent years, PFAS has become a major global health concern due to their widespread ecological presence, exceptional stability, and growing evidence of toxicity in both humans and animals. Among the various PFAS compounds, perfluorooctanoic acid (PFOA) and perfluorooctane sulfonic acid (PFOS) are the most common, and they have received extensive global documentation and research. While this review primarily focuses on these compounds,

it also includes relevant discussions about related compounds as deemed appropriate (Sinclair Georgia M., 2020).

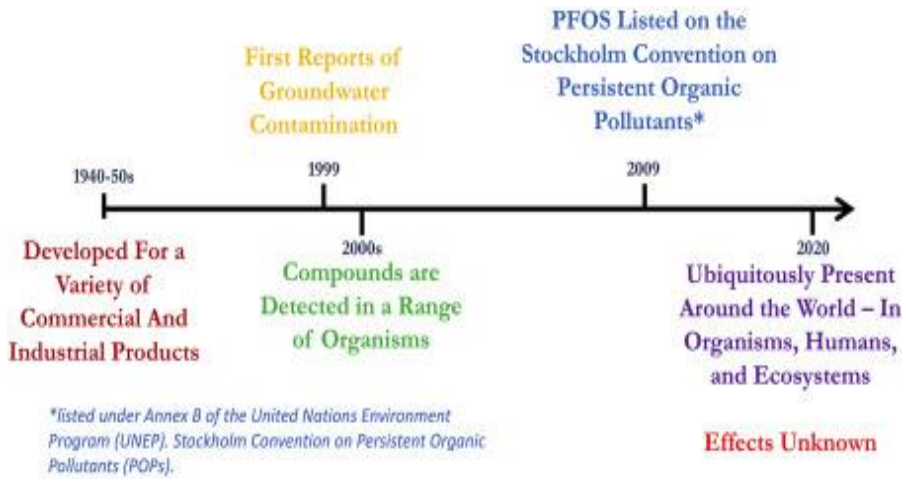

Figure 2-1.History of PFAS (Sinclair et al 2020)

2.2.1Formation of PFAS

The initial definition of PFAS referred to them as aliphatic compounds containing one or more carbon atoms, where all hydrogen atoms are replaced by fluorine atoms, resulting in a perfluoroalkyl group (–CnF2n+1–). Ten years later, the Organization for Economic Co-operation and Development (OECD) provided a broader and more user-friendly definition. This definition classifies PFAS as fluorinated substances with at least one fully fluorinated methyl or methylene carbon atom. Consequently, with a few exceptions, any chemical containing a perfluorinated methyl group (–CF3) or a perfluorinated methylene group (–CF2–) is considered PFAS. This updated definition, known as OECD2021, eliminates the need for the structure to be completely aliphatic, requiring only that the fully fluorinated methyl or methylene group be saturated and aliphatic (OECD, 2021) (Gaines Linda G.T, 2023).

OECD2021 includes approximately 38,000 structures currently available in the USEPA's public version of the Computex Chemicals Dashboard and over 6.1 million structures in PubChem. These databases are constantly growing with new registrations, indicating a

continuous increase in the number of structures meeting this simple definition (Gaines Linda G.T, 2023).

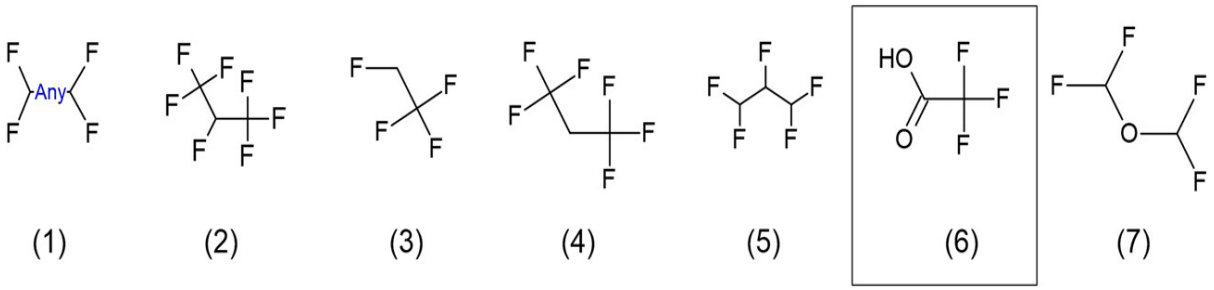

Figure 2-2 Various structures of PFAS (Gaines Linda G.T, 2023)

Table 2-1 -Historical inventory of recorded PFAS) (Gaines Linda G.T, 2023)

Version	Date	Description	Number of structures
PFASSTRUCTv1	2018	(1) Formula must contain 4–1000 fluorine atoms; (2) structure must contain two adjacent CF2 groups, either in a chain or in a ring system; (3) fluorine-to-carbon ratio (#F/#C) must be ≥0.5; and (4) removal of Markush structures, charged species (e.g., anions), free radicals, and deuterium- and C13-labeled chemicals	4357
PFASSTRUCTv2	2019	R–(CF2)–C(F)(R′)R″, both the CF2 and CF moieties are saturated carbons and none of the R groups (R, R′ or R″) can be hydrogen (TSCA2021)	6648
PFASSTRUCTv3	2020	Structures containing one of the substructures in Figure 2	8163
PFASSTRUCTv4	2021	Structures containing one of the substructures in Figure 2 excluding Substructure 6	10 776

CF2, perfluorinated methylene group; TSCA, Toxic Substances Control Act

2.3 PFAS properties, uses, sources, and their distribution into the environmental compartments

PFAS are widespread in the environment, but current remediation methods and technologies have been ineffective in breaking them down. These substances are found in groundwater, impacting both animals and humans. PFAS also contaminate soil, plants, and even drinking water.

2.3.1 Effects on humans from PFAS

PFAS encompasses a broad array of contemporary chemical compounds that are causing concerns regarding human and environmental health. These substances are defined by their fluorine content, particularly featuring either a perfluorinated methyl group (−CF3) or a perfluorinated methylene group (−CF2−) (Sadia Mohammad, 2023) making them a varied group of chemicals. PFAS can be found in drinking water due to their widespread use and behavior in the environment. Because of their extensive production and use, as well as their ability to persist, move through the environment, and build up in living organisms, PFAS is causing significant concerns, which could have a global impact. High levels of PFAS have been detected in various environmental areas, including food, consumer goods, human biological fluids (such as milk and blood), and both drinking and surface waters. (Sadia Mohammad, 2023)

2.3.2 Sources of PFAS emissions

PFAS are continuously emitted into the air from various sources, including industrial activities like fluoropolymer production, building construction, food packaging, textile manufacturing, medical device production, and the professional use of firefighting foams, printing inks, and paints. Furthermore, PFAS are consistently released through the use and disposal of consumer goods such as cosmetics, personal care products, household items, and materials used for food storage and processing (Emiliano, 2022).

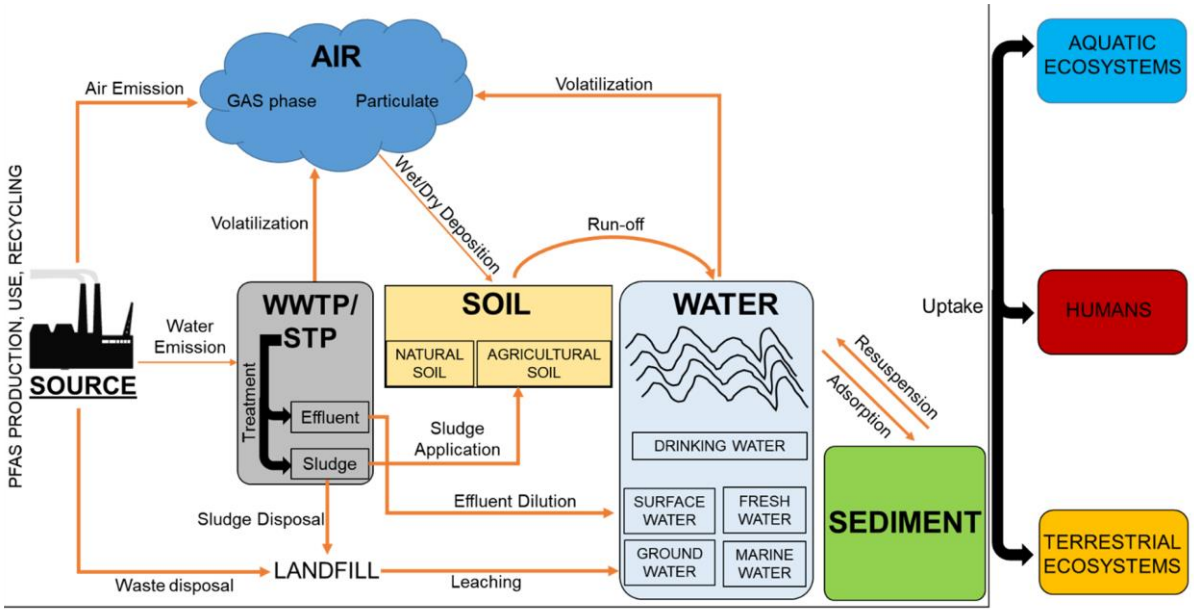

Figure 2-3 PFAS emission cycle (Emiliano, 2022)

2.3.3 PFAS occurrence in the atmosphere

Many PFAS compounds have low vapor pressure, low Henry's law constant, and high boiling points, making them not easily evaporated. However, some neutral compounds such as perfluoro octane sulfonates (FOSAs) or sulfamidoethanols (FOSEs), as well as compounds like fluorotelomer alcohols (FTOHs) or acrylates (FTACs), can evaporate to some extent. These substances can enter the air. One study of the atmosphere above the northern South China Sea found four main types of PFAS molecules: FTOHs, FTAs, FOSAs, and FASEs, with an average total concentration for 54.5 pg/m^3. Even PFAS compounds that do not evaporate easily can stick to organic matter, making it easier for them to get into the air after sticking to particles in the atmosphere. Research in Japan, China, and India looked at differences in PFAS stuck to air particles of different sizes particles starting range from 0.1 to 10 μm or PM10-PM0.1 at different times of the year (Emiliano, 2022). The movement of PFAS compounds through the air carries important implications for their journey to various parts of the environment and receptors. Both wet and dry deposition processes play a substantial role in PFAS entering aquatic and terrestrial ecosystems. Overall, these discoveries emphasize that the atmospheric dispersal of PFAS is a significant pathway through which these substances can spread to

humans and potentially other biological receptors located far from where they are emitted (Emiliano, 2022).

2.3.4 PFAS occurrence in groundwater

The Earth's surface accounts for approximately 30% of the world's freshwater resources. Groundwater plays a vital role in regulating water levels and flow in rivers, lakes, and wetlands, providing a natural resource for wildlife and plant life. Additionally, groundwater is crucial for socio-economic reasons, as it is the primary source of water for industrial activities, agriculture, and drinking purposes. Globally, various sources of contamination and pathways have been identified, leading to a substantial impact on human exposure to PFAS through groundwater reservoirs

2.3.5 PFAS occurrence in drinking water

Pure drinking water is a major source of PFAS exposure for humans, with even small concentrations of PFAS present in water potentially resulting in substantial accumulations in the bloodstream over an individual's lifetime. Research suggests that continued consumption of PFOA through drinking water could result in blood concentrations up to 100 times higher than the levels found in the water because the substance is slowly eliminated and accumulates in the body, especially when compared to other animal species. Numerous research studies have identified PFAS contamination in drinking water in several countries outside the EU. For example, an organization conducted a comprehensive analysis from 2013 to 2015 as part of the US EPA UCMR3 program, elevated levels of PFOA and PFOS were detected in water supplies serving nearly 6 million residents, surpassing the recommended limit of 70 ng/L. This has raised serious concerns about potential adverse effects, especially given the lack of data on personal wells, which supplied drinking water to up to one-third of the US population. (Emiliano, 2022)

2.3.6 PFAS occurrence in soil and plants

In most cases, PFAS compounds make their way into the environment via underground pathways and predominantly impact soils. They undergo various processes before moving into other areas such as surface or groundwater systems. Sources of PFAS contamination in terrestrial environments include atmospheric deposition, AF discharge, using polluted water for irrigation, and applying biosolids or municipal sludge in agriculture. PFAS emissions raise significant concerns for human food safety, notably when fluoropolymer manufacturing facilities near agricultural areas. This proximity can lead to high concentrations of PFAS in the soil and edible crops, highlighting the importance of considering PFAS presence in soil due to atmospheric dispersion (Emiliano, 2022).

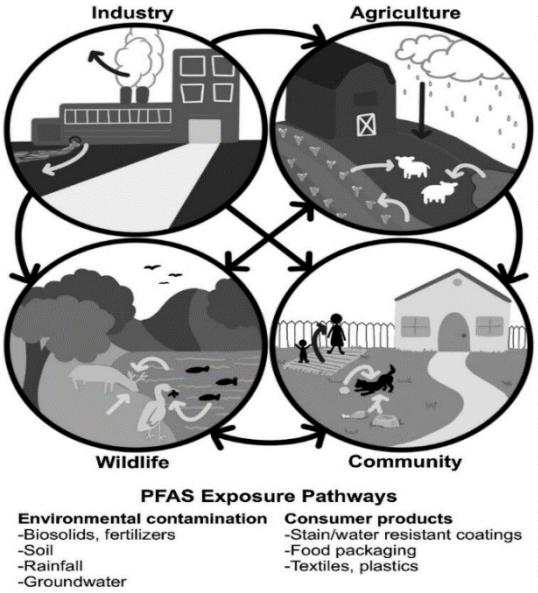

Figure 2-4 PFAS Exposure pathways (Emiliano, 2022)

The contamination of agricultural soil by PFAS can come from multiple sources. This includes direct exposure from fluorochemical industrial plants or the use of aqueous film-forming foams. PFAS can also infiltrate the soil through the application of contaminated biosolids or

irrigation water. Human exposure to PFAS commonly occurs through the consumption of contaminated food and drinking water, particularly fish, meat, and eggs. Numerous studies have examined the risks linked to PFAS exposure through polluted food and water sources. Furthermore, if the water supply comes from an area contaminated with PFAS, drinking water can become a significant pathway of exposure. The different ways PFAS enter the environment and what happens to them afterward is shown in Figure 2-5. STP refers to a sewage treatment plant.

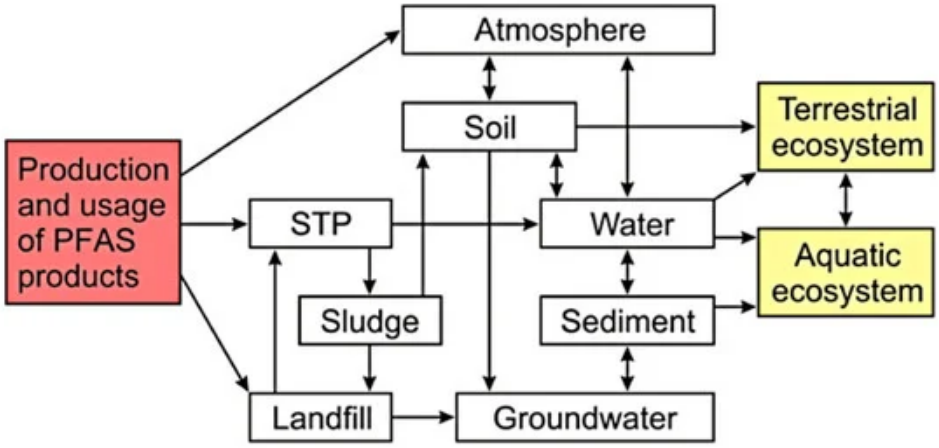

Figure 2-5 Production of PFAS Product (Bonato, et al., 2020)

2.3.7 PFAS human exposure and the potential effects on human health

The pathways through which PFAS emissions from primary or secondary sources reach humans, including workers and the general population, are well recognized. Major exposure routes include inhaling air and dust particles, consuming contaminated food and water, and absorbing the substances through the skin. Although there are still some gaps in our knowledge, it is widely recognized that dietary intake and drinking water are the primary pathways of exposure for the general population, whereas inhalation and skin contact are more important for occupational exposure. The likelihood of PFAS causing various adverse health effects depends on factors such as exposure conditions (including the amount, duration, and route of

exposure) and the characteristics of the exposed individuals (such as age, sex, ethnicity, and health). PFAS impacts a range of biological functions in both females and males, including disrupting endocrine function, affecting fertility, and influencing body weight, and thyroid function, PFAS exposure has been linked to developmental effects in children, such as behavioral changes or early puberty, and in newborns, including lower birth weight. Prolonged exposure to PFAS in the general population has also been associated with an increased risk of kidney, prostate, and testicular cancer, as well as disruptions in cholesterol metabolism and a weakened immune response to infections (Bonato, et al., 2020).

The Po Valley, known for its lush agricultural landscape, is a key contributor to the prosperity of the Veneto region. In Europe and Italy major area of vegetable, fruits and wine to be produced, significantly impacting the region's economy. Italy stands out in terms of agricultural water usage in Europe, with a substantial portion sourced from both surface and groundwater reservoirs. In 2013, the discovery of PFAA contamination in the Veneto region, linked to emissions from a fluorochemical plant in Vicenza province, raised concerns. The contamination was highlighted in the 2015 Veneto Region report, which identified areas exceeding safe limits for PFOS, PFOA, and other PFAS in drinking water. However, the report did not provide specific PFAS concentration levels. It's important to note that certain areas marked in white were excluded from the selection outlined in the Veneto Region Report.

Municipalities in the Veneto region is classified as contaminated (dark grey) or uncontaminated (light grey) according to the Italian National Health Institute's (ISS) performance limits for drinking water. In many municipalities (white), no analyses were conducted.

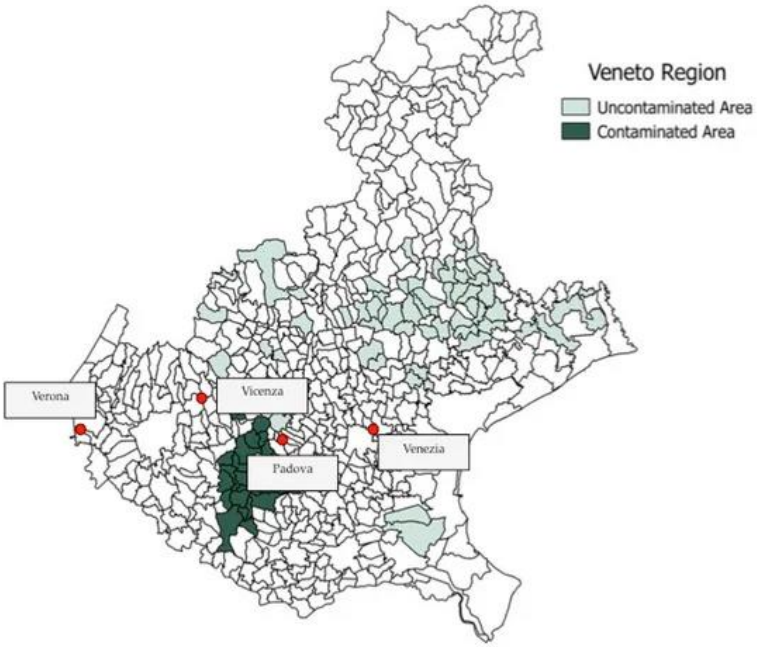

Figure 2-6 Municipalities in the Veneto region (Bonato, et al., 2020)

2.3.8 Oxidative stress in human health due to PFAS pollution

Exposure to PFAS has been connected to various negative impacts on human health, such as disturbances in thyroid function, kidney health, and metabolic processes. Since PFAS can remain in the human body and the environment for extended periods, it is crucial to carry out biomonitoring studies in populations with long-term exposure. These studies and follow-up research could offer crucial insights into the health risks linked to this group of chemicals.

In adults, PFAS disrupts reproductive functions, steroid hormones, adipokines, asthma and allergies, and maternal fatty acids. It is generally thought that adult lung tissue accumulates the highest levels of PFAS, though PFOS primarily accumulates in the liver and PFOA in bone structures. Importantly, PFOA, PFOS, PFNA, PFDA, and PFUnA have been found in all human tissues.

2.4 Methods of removal of PFAS

There are several methods to remove PFAS such as:

1. Destruction techniques.
2. Adsorption methods: using activated carbon, biochar or other adsorbents.
3. Biological methods using microbiological and fungal methods.

A summary of removal techniques is presented in Table 2-4.

Table 2-2 Removal technologies of PFAS from the environment (Meegoda Jay N., 2022)

Technologies	Process	Advantages	Disadvantages	Sources
Adsorption	Removal of PFAS compounds via adsorption to selective materials of adsorbing potential (e.g., Biochar, Resin, and modified clays)	Low operational cost and uses several materials which are commercially available	Ineffective for short-chain PFAS removal Interfere with other pollutants May require a large quantity of the adsorbent may be required, which causes a change in the land use.	Zhang et al., 2011
Filtration	Uses Reverse osmosis or Nanofiltration to remove PFAS compounds	Effective under a wide range of pH	Expensive PFAS molecular weight dependent Creates high concentration waste	Tang et al., 2007
Thermal	Vaporizing the contaminants through increasing temperature to about 600 −1,000◦C	High destruction potential of the PFAS compounds	Time-consuming, high-cost and energy-intensive approach. Disturbs the soil and the ecosystem.	Yamada et al., 2005
Chemical oxidation/ reduction	Using chemical oxidants/reducing agents for the abiotic breakdown of contaminants	Potential for PFAS mineralisation; effective in PFOA remova	Very expensive as it requires a large volume of chemicals and centralized equipment. Not applicable to treat all PFAS compounds. Short-chain PFAS could result. Interferes with other contaminants.	Yates et al., 2014; Arvaniti et al., 2015
Soil washing	Detaching PFAS from the soil by washing with water	Requires low technology Land reuse could be possible.	Expensive and time-consuming. Contaminated water results.	de Bruecker, 2015
Bioremediation	Use of biological agents (e.g., Microorganisms and Plants) to	Simple, cost-effective, and environmentally safe (Green) approach	Limited evidence that PFAS can be degraded. It could take a long time due	Presentato et al., 2020

breakdown or accumulate PFAS compound	to the slow biodegradation of PFAS.

2.4.1 Destruction techniques for PFAS

Technologies like electrochemical oxidation, plasma, photocatalysis, sonolysis, supercritical water oxidation, and thermal degradation can remove PFAS to prevent human exposure. Certain technologies are more effective for treating high-concentration streams of long-chain PFAS, while others perform better in low-volume systems. Capital and maintenance costs, along with long-term energy consumption, are also important factors to consider. A summary of destruction techniques is presented in Table 2-2.

Table 2-3 Summary of the main advantage and disadvantage of the PFAS destructive technologies (Meegoda Jay N., 2022)

TECHNOLOGY	ADVANTAGES	DISADVANTAGES
ELECTROCHEMICAL OXIDATION	Effective for long-chain PFAS. Efficient for highly concentrated PFASs. Effective for low-volume PFASs. Low environmental impact. Does not require pretreatment.	Widescale application. Inefficient for short-chain PFASs. Electrodes are expensive. Reduced electrode lifetime. High energy consumption. Toxic by-products. Forms short-chain PFAS
PLASMA	Effective for long-chain PFASs. Effective for short-chain PFASs. Low energy consumption. No chemical additives are needed. Short treatment time. Effective for highly concentrated PFASs. Effective against co-contaminants.	Affects water's pH, making it acidic. Forms short-chain PFASs. Its mechanism is not well understood. Longer time for short-chain treatment. The addition of chemicals is required. Nontargeted reactions can result in longer treatment time.
PHOTOCATALYSIS	Low energy consumption. Performed at ambient temperatures. Sustainable technology. It can be recycled.	Low degradation efficiency. Inefficient for sulfonic groups. Toxic intermediate products. Additional treatment is needed.
SONOLYSIS	Effective for long-chain PFASs. Effective for short-chain PFASs. Effective in soils and liquids.	Widescale application. High energy consumption. Its mechanism is not well understood.

SUPERCRITICAL WATER OXIDATION	Effective for long-chain PFASs. Effective for short-chain PFASs Low environmental impact. Relatively quick treatment time	Not economically viable for large volumes. Affects water's pH, making it acidic. Corrosion of the reactor. Toxic intermediate products.
THERMAL DEGRADATION/ INCINERATION	Widescale application. Reduced capital cost. Effective for long-chain PFASs.	Toxic intermediate and final products. High environmental impact. Air and soil contamination. Toxic emission.

In one paper, a plasma reactor was used to break down poly- and perfluoroalkyl substances (PFAS) in leachate samples obtained from three different locations (Singh, Brown, Thagard, & Holsen, 2021). The results of their study suggest that plasma-based technology was an effective approach for remediation of PFAS-contaminated landfill leachates (Singh, Brown, Thagard, & Holsen, 2021).

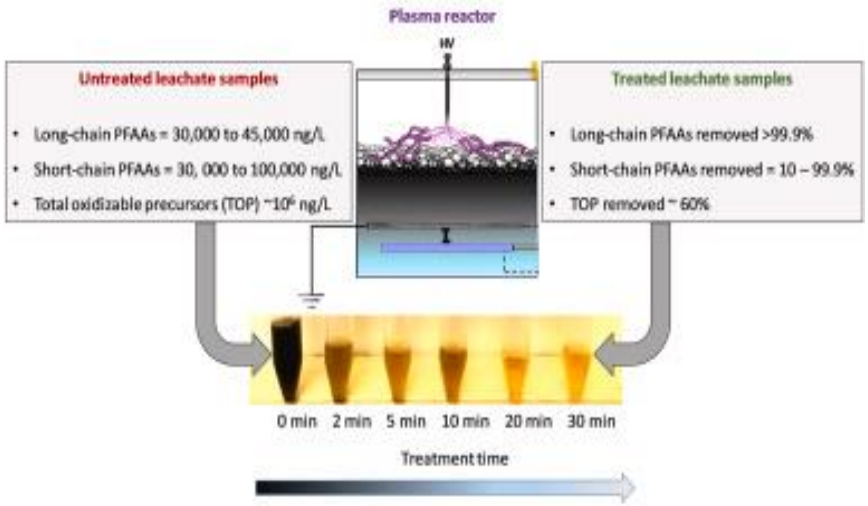

Figure 2-7 Plasma reactor (Singh, Brown, Thagard, & Holsen, 2021)

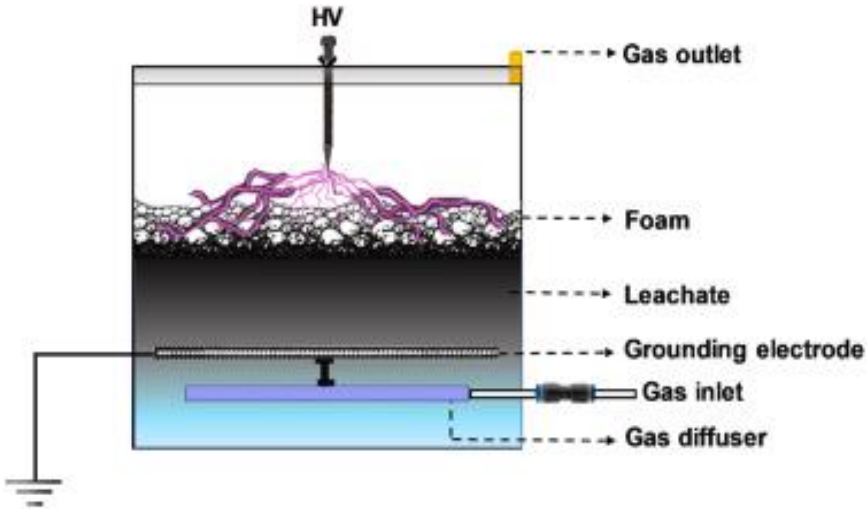

Figure 2-8 Schematic of the plasma reactor (Singh, Brown, Thagard, & Holsen, 2021)

Research conducted by Jianhua Zhang et al. focused on the efficiency of eliminating PFAS using ferric nanoparticles formed in situ through ozonation. The study involved testing synthetic contaminated water with PFAS concentrations ranging from 8.33 to 133 µg/L, pH levels from 3 to 7.5, and ozone bubbling times from 15 to 45 seconds. The ferrous dose, pH, and ozone bubbling time influenced the ferric nanoparticles' size. The maximum PFAS removal reached was 44% under particular conditions, including a PFAS concentration of 8.33 µg/L, a ferrous dose of 40 µg/L, a pH of 6.2, and an ozone bubbling time of 45 seconds. Furthermore, the PFAS solid phase loading on ferric nanoparticles surpassed that of commonly used adsorbents. The study also revealed that it was not feasible to simultaneously achieve both the highest PFAS removal and the highest PFAS solid phase loading on ferric nanoparticles under the experimental conditions tested (Belkouteb, Franke, McCleaf , Kohler, & Ahrens, 2020).

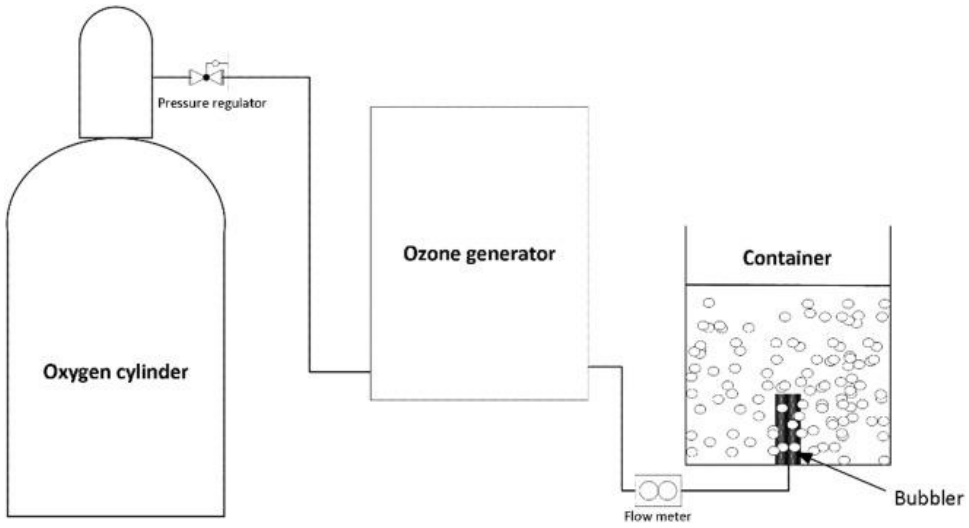

Figure 2-9 Experimental setup

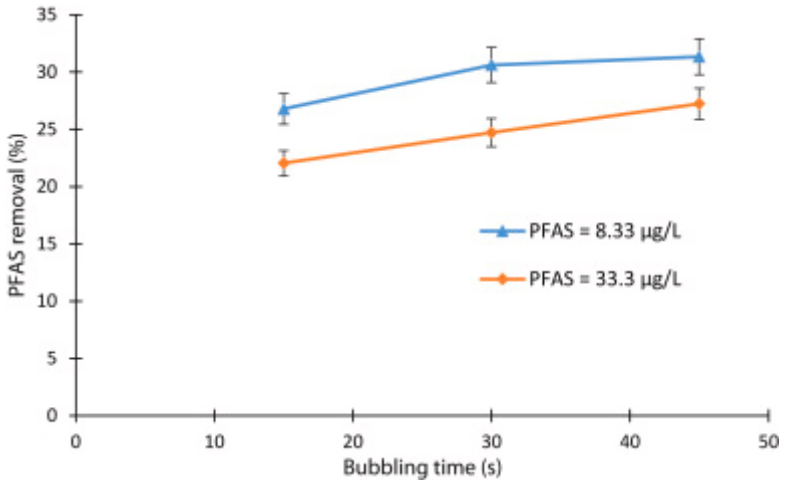

Figure 2-10 PFAS removal varies with the original PFAS concentration at different bubbling times (mass ratio of FeSO4/PFAS = 1:1.8 ± 0.2) (Zhang, et al., 2021).

2.5 Biochar and Other Sorbent Materials

Biochar is a solid material that is produced through the process of biomass pyrolysis, which has been practiced for thousands of years (Arfin, Bushra, & Mohammad, 2016). It is commonly known as charcoal, particularly when derived from woody biomass. The process of pyrolysis involves subjecting the biomass to high temperatures, leading to the breakdown of the organic matter and the creation of biochar. It begins with the drying phase of the biomass, followed by the thermal breakdown of the fuel in the absence of external oxygen, ultimately resulting in the

formation of a solid residue known as biochar (Weber & Quicker, 2018). The amount of product that can be obtained from the pyrolysis of a particular biomass depends on a range of process variables such as temperature, residence time, heating rate, and biomass characteristics (Weber & Quicker, 2018).

Adding biochar to soil can significantly modify the physical characteristics of the system, including depth, texture, structure, porosity, and consistency, including bulk surface area, pore-size distribution, particle-size distribution, density, and packing. As a result, the influence of biochar on soil physical properties can directly affect plant growth, as it influences factors such as the depth of root zone penetration and the availability of air and water, which are largely determined by the physical composition of the soil (Downie, 2009).

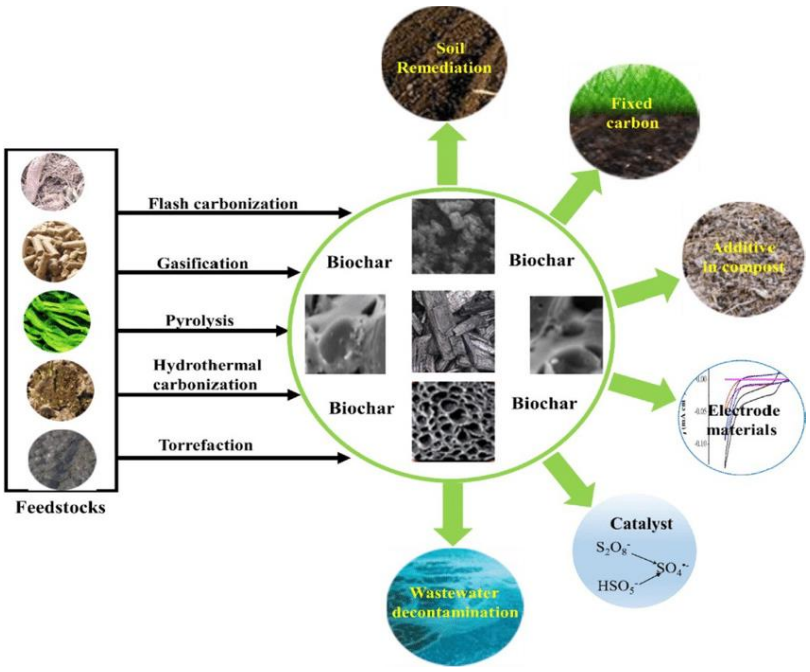

Figure 2-11 schematic diagram of biochar from different feedstock

Biochar is used in various fields such as medicine, filtration, and separation. When biochar undergoes an activation process, it is often referred to as "activated carbon." This activated

carbon has a wide range of applications due to its increased porosity and large surface area, making it effective for adsorption and purification processes in various industries (Arfin, Bushra, & Mohammad, 2016).

(1)

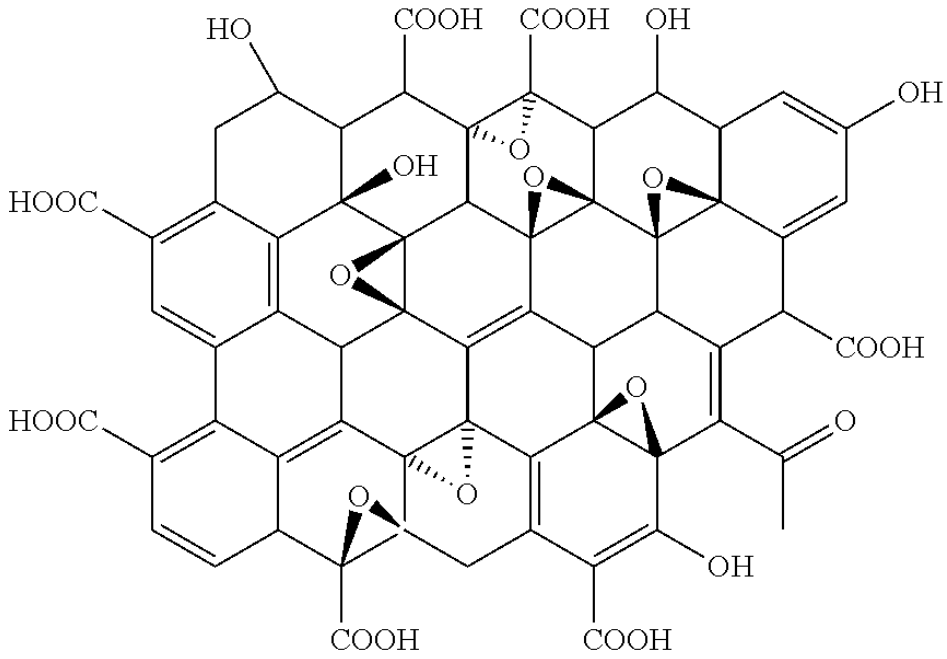

Figure 2-12 Chemical structure of char (Arfin, Bushra, & Mohammad, 2016)

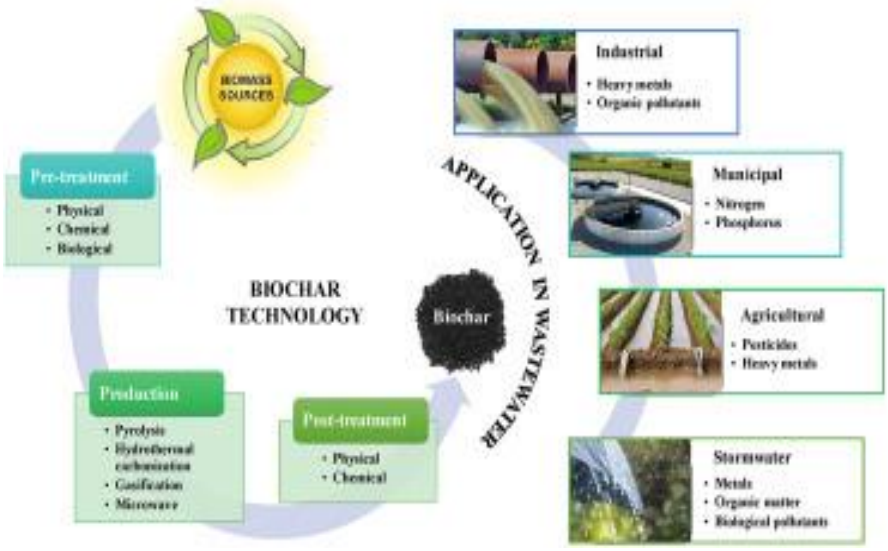

Figure 2-13 application of biochar in wastewater (Xiang, Zhang, & Chen, 2020)

Because biochar is a highly porous carbonaceous material, with a significant surface area and numerous functional groups, it is an effective adsorbent for removing a wide range of contaminants. As a result, the significance of biochar as a remedial solution for tackling pollutants in industrial and agricultural settings has increased significantly (Xiang, Zhang, & Chen, 2020) (Wang et al., 2017a).

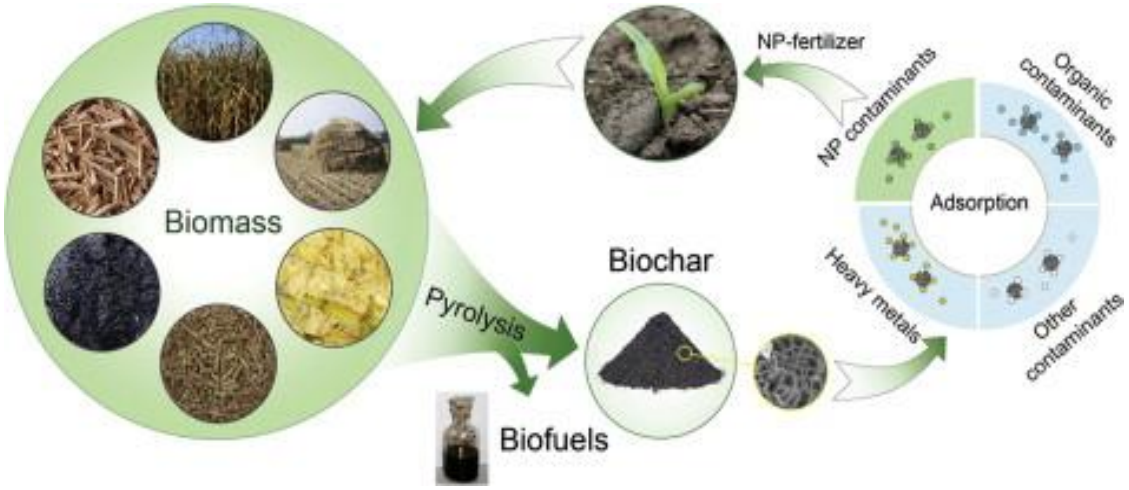

Figure 2-14 Use of biomass to produce biochar and biochar applications (Tan, et al., 2015)

Research by Cerlanek and Liu (2024) focused on examining the use of wood-derived biochar from construction and demolition waste for reducing PFAS in landfill leachate (Cerlanek, et al., 2024). In batch tests, one type of biochar gave 29% reduction in PFAS compared to control conditions. However, columns packed with this biochar consistently produced leachates with PFAS levels 50% to 80% higher than control columns. Columns with another type of biochar initially reduced PFAS concentrations by 44% compared to controls, but subsequent weeks showed similar concentrations. The study suggests that using biochar derived from wood construction and demolition waste did not significantly remove PFAS from landfill leachate (Cerlanek, et al., 2024).

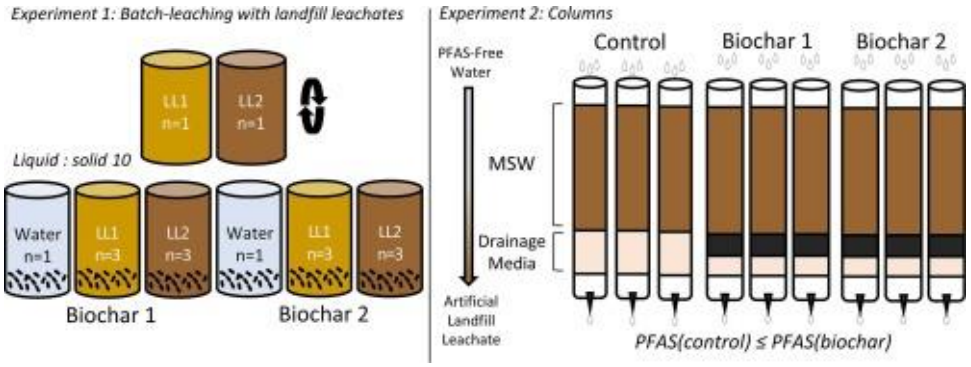

Figure 2-15 Batch leaching and the column (Cerlanek, et al., 2024)

In a recent study, Du et al (2015) presented research which is focused on the removal of perfluorinated carboxylates from wastewater containing perfluorooctanesulfonyl fluoride using activated carbons and resins. It was discovered that the high concentration of inorganic ions in the wastewater resulted in greater PFAS removal by biological activated carbon (BAC) in actual wastewater compared to simulated solutions (Du, et al., 2015). Commercially available ion exchange resins like IRA958 and IRA67 can adsorb perfluorooctanoic acid (PFOA) and perfluorooctane sulfonate (PFOS) at a level of up to 5 mmol/g (Singh, Brown, Thagard, & Holsen, 2021). In another paper the adsorption of PFCAs by activated carbon and ion exchange was hindered by the presence of organic compounds in wastewater. Spent BAC and IRA67 could be effectively regenerated using an ethanol solution or a NaCl/methanol mixture, with IRA67 maintaining stable PFCA removal across five adsorption cycles (Singh, Brown, Thagard, & Holsen, 2021).

Zimmerman and Hale (2019) conducted a study on the effectiveness of customized biochars in remediating soils contaminated with organic and inorganic pollutants, particularly per and polyfluorinated alkyl substances (PFAS). They examined waste timber biochar (BC), coconut shell activated biochar (ABC), and wood shrub iron-enriched designer biochar (Fe-BC) across varying levels of total organic carbon (TOC) in the soil. The study involved the application of six different doses of BC and ABC, and it suggested that the use of specially crafted "designer" biochars, which may include processes like iron enrichment or activation, should be carefully

considered based on the soil's TOC, contaminant types, and remediation goals (Silvani, et al., 2019).

In a recent study, biochar derived from reed straw (RESCA) for removing short chain perfluoroalkyl acids (PFAAs) from drinking water and groundwater was investigated (Liu, Wu, Lyu, & Li, 2021). While granular activated carbon (GAC) is commonly used for this purpose, it has limitations in eliminating short-chain PFAAs. The researchers found that RESCA had removal efficiencies of over 92% for short-chain PFAAs at environmentally relevant concentrations (Liu, Wu, Lyu, & Li, 2021).

PFAS has been extracted from water using permanently confined micelle arrays (PCMA). Equilibrium was reached within five minutes for PFOS, PFHxS, and PFBuS. The impact of pH and salt concentration on the sorption of PFOS was found to be minimal, and the PCMAs maintained consistent PFAS removal efficiency even after five regeneration cycles (Wang, Lu, Shih, Wang, & Li, 2014).

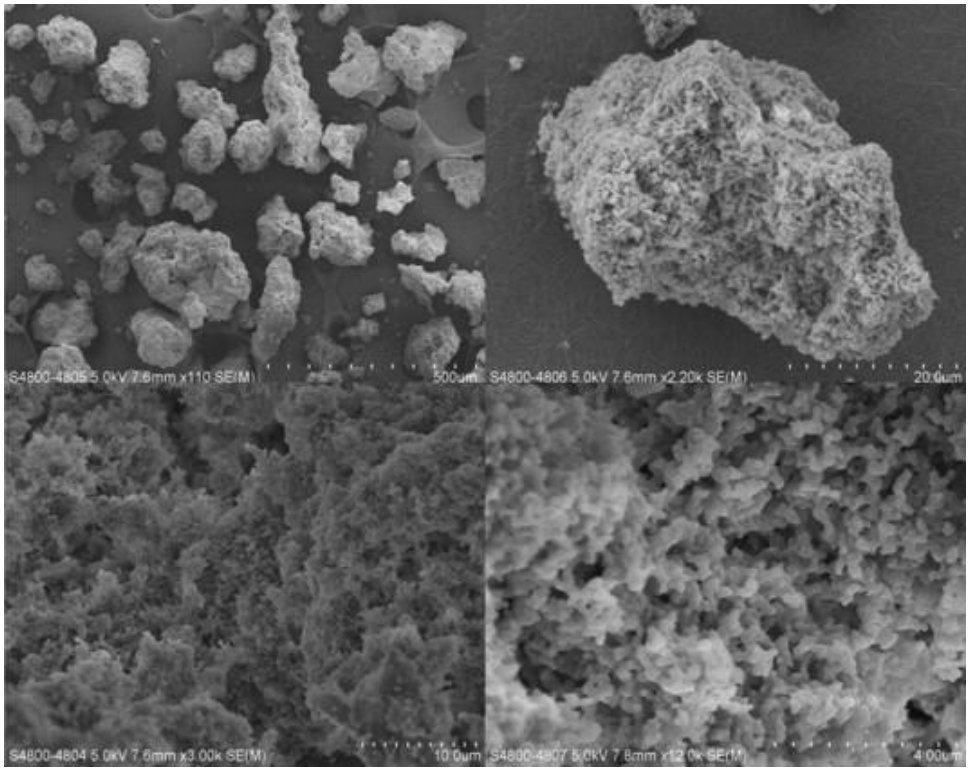

Figure 2-16 The SEM pictures of the as-made PCMA. The results demonstrated the formation of macropore and macroporous channels in the new materials (Wang, Lu, Shih, Wang, & Li, 2014).

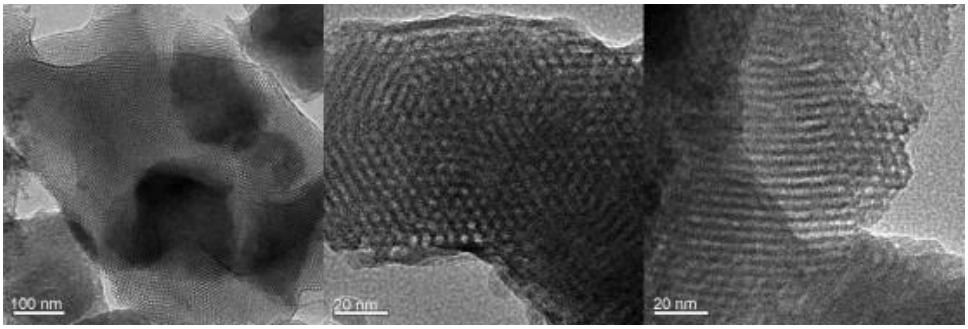

Figure 2-17 The TEM pictures of the as-made PCMA. The results showed the highly ordered hexagonal mesoscopic organization of cylindrical micelle was formed (Wang, Lu, Shih, Wang, & Li, 2014).

Dalahmeh et al. (2019) investigated the feasibility of utilizing biochar filters as a substitute for, or in conjunction with, sand filters in the removal of per- and poly-fluoroalkyl substances (PFASs) from wastewater within on-site treatment systems. They assessed the concentrations and removal of different PFASs over a 22-week period using four distinct column filter treatments: biochar without biofilm (BC-no-biofilm), biochar with active biofilm (BC-active-biofilm), biochar with inactive biofilm (BC-inactive-biofilm), and sand with active biofilm

(Sand-active-biofilm) (Dalahmeh, Alziq, & Ahrens , 2019). The most effective approach for using biochar filters was as a second-stage treatment (or post-treatment) step, specifically targeting the removal of PFASs after the removal of organic matter (Dalahmeh, Alziq, & Ahrens , 2019).

Table 2-4 Physical characteristics of biochar and sand filters

Parameter	Biochar (BC-active-biofilm, BC- inactive-biofilm and BC- no-biofilm)	Sand-active-biofilm
Particle size distribution (mm)	1–5	1–5
Effective size (mm)	1.5	1.4
Uniformity coefficient	2.1	2.2
Total porosity (%)	72–74	40
Specific surface area ($m^2\ g^{-1}$)	184	0.14
Bulk density ($kg\ m^{-3}$)	187	1700

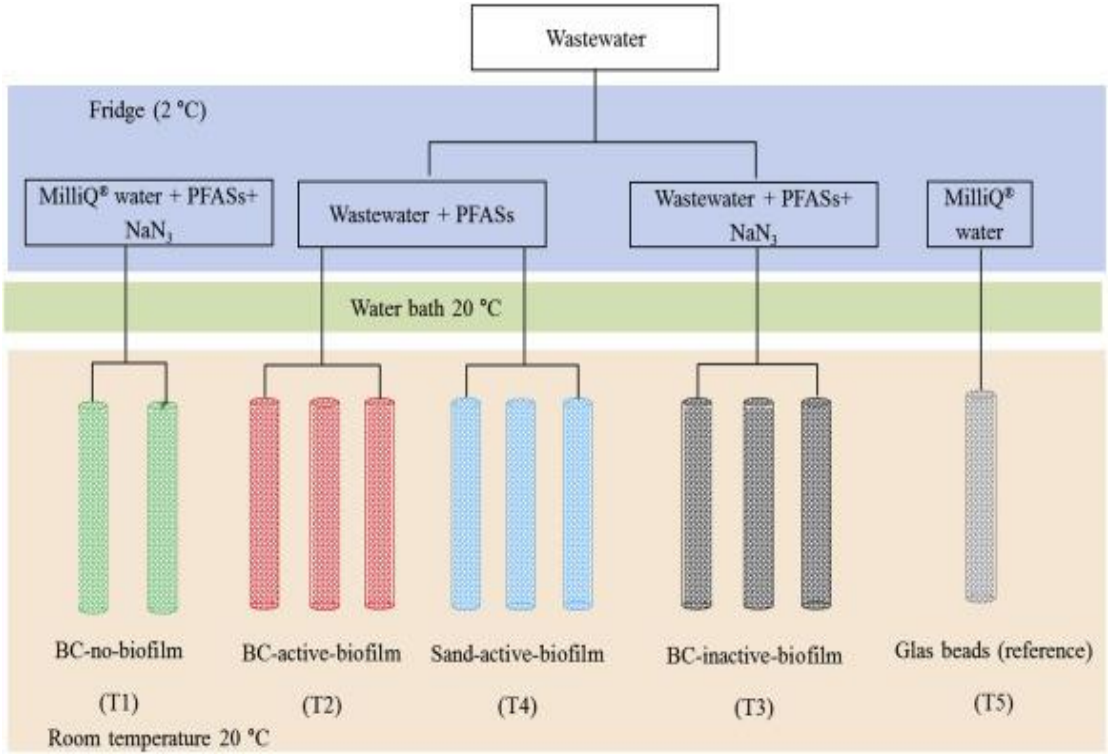

Figure 2-18 Schematic diagram of the column experiments using biochar (BC) with no biofilm (T1, n = 2), active biofilm (T2, n = 3) and inactive biofilm (T3, n = 3), sand with active biofilm (T4, n = 3) and a glass bead

filter as a filter blank (T5, n = 1). PFASs = per- and polyfluoroalkyl substances (Dalahmeh, Alziq, & Ahrens , 2019)

The effectiveness of a full-scale drinking water treatment plant in Uppsala, Sweden, in removing 15 per- and poly-fluoroalkyl substances (PFASs) over two years (2015–2017) was investigated. The study revealed that the efficiency of removing the five frequently detected PFASs depended on factors such as the operational time of granular activated carbon (GAC) filters, GAC type, and surface loading rate. Results demonstrated that "young" GAC filters exhibited higher removal efficiency (92–100%) compared to "old" GAC filters (7.0–100%). Manipulating flow rates in different operational-age GAC filters resulted in variations in PFAS and organic matter removal, with decreased flow rates leading to increased PFAS removal efficiency. Additionally, an analysis of costs emphasized the significance of treatment goals and GAC regeneration costs in determining overall GAC operation costs (Zhi & Liu, 2015).

Using activated carbon in removing PFAS from polluted water has limitations such as prolonged equilibrium times, ineffective capture of short-chain PFAS, and reduced adsorption in the presence of other organic compounds. Militao, Roddick, & Fan (2023) produced biochar-alginate beads which were not affected by pH and the presence of natural organic matter for removing PFOS or PFBS.

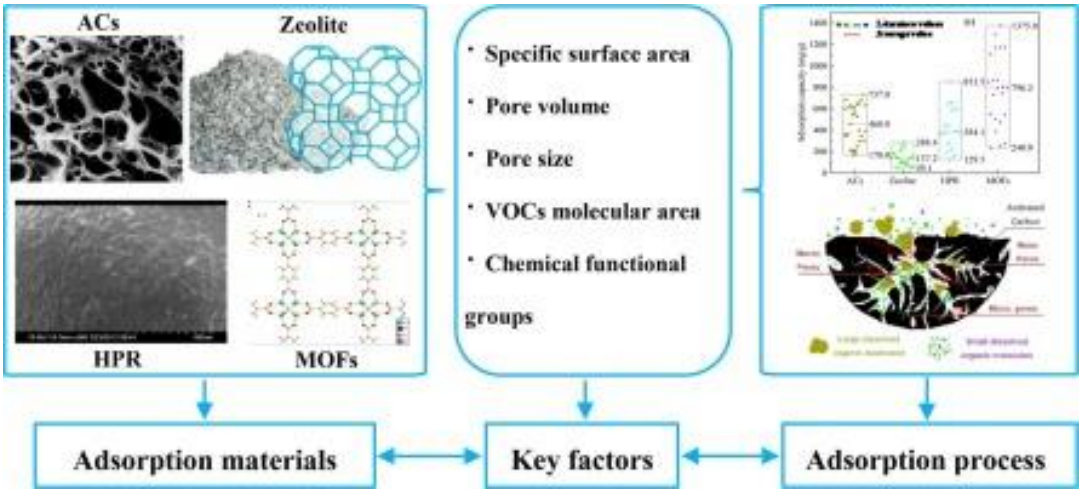

Figure 2-19 Adsorption capacity for PFAS (Li, Yang, Wang, Yan, & Ran, 2020)

One study tested the adsorption capacity of four different types of activated carbon produced from bituminous coal for PFAS in groundwater using rapid small-scale column tests (RSSCTs). The adsorption capacity based on the half breakthrough bed volume (BV50), increased with the hydrophobicity of PFAS at a given pH (Log Dow) for one of the activated carbons. Activated carbon with three different particle sizes (0.13, 0.17, and 0.20 mm) exhibited similar breakthrough profiles for PFAS, suggesting that intraparticle diffusivity stayed consistent regardless of the adsorbent's diameter, probably due to very low concentrations of PFAS and the bulk of the PFAS adsorbing to the outer surface of activated carbon.

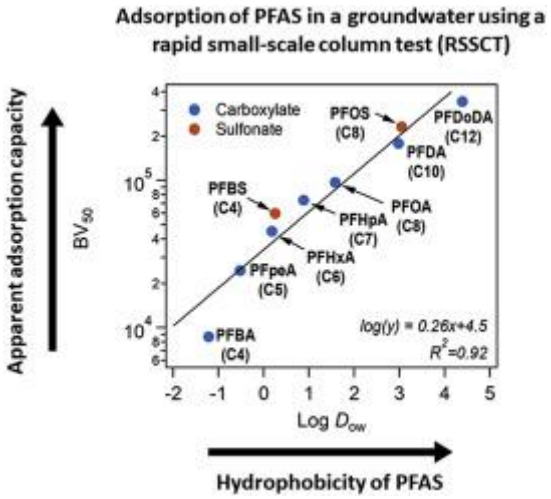

Figure 2-20 Adsorption of PFAS in a groundwater using a rapid small-scale column test (RSSCT)

2.6 Bioremediation of PFAS

Biodegradation of PFAS involves enzymes that directly remove fluorine atoms from PFAS by adding oxygen across the F-C bond (oxidation) or by adding electrons (reduction). While there have been no reports of removal of fluorine atoms from PFAS, there are examples of defluorination of mono-fluorinated compounds by many bacteria. *Pseudomonas* isolated from environments contaminated with PFAS were able to remove 28-32% of PFAS within 10 days. PFAS can be bioremediated using certain bacterial strains of *pseudomonas, acidimicrobium* and *gordonia* which will remove between 32 to 75% of the PFAS over periods from 2-100

days. (Shahsavari Esmaeil, 2021) Research examining mycoremediation of PFAS using fungi is limited to wood-rotting fungus *Phanerochaete chrysosporium* where it removed 50% of 2-(Perfluorohexyl)ethanol (6:2 FTOH) within 28 days.

Fungi belong to a group of eukaryotic organisms that includes microorganisms like yeast, molds, and mushrooms. Due to their often tiny structures, most fungi go unnoticed. This diverse group also includes species that form symbiotic relationships with plants and animals, as well as those that act as parasites. They are essential decomposers, breaking down dead organic matter and recycling nutrients back into the environment. Without fungi, many ecosystems would struggle to sustain themselves. In addition to their ecological roles, fungi are also important in various industries. Some fungi benefit plants, helping them absorb nutrients through symbiotic relationships, like in mycorrhizae. However, others can be harmful, causing diseases in plants, animals, and even humans.

Fungi are known to degrade lignin, one of the most recalcitrant natural compounds along with many toxic natural and xenobiotic compounds including DDT and DDE, organophosphates, pesticides, including chlorpyrifos and polychlorinated biphenyls (Beaudette et al., 2000) and polyaromatic hydrocarbons (Moghimi et al., 2017). White-rot fungi in particular have been successful in remediating organic toxins including polychlorinated biphenyls, organophosphate pesticides and polycyclic aromatic hydrocarbons (Shahsavari Esmaeil, 2021). They do this by secreting a laccase enzyme which is involved in the oxidative degradation of phenols present in lignin and toxic compounds. Basidiomycete fungi are versatile in their ability to degrade persistent chemicals. In New Zealand, *Trametes versicolor* and *Pleurotus pulmonarius* (oyster mushroom) have been trialled as a means to remove PCP and dioxins from soil (Thwaites et al 2006) and sediment from former mill sites around New Zealand including contaminated sediment from the Kopeopeo canal in Whakatane (Health Research Council 2012). Full scale bioremediation of approximately 32,000 tonnes of dioxin contaminated

sediment from the Kopeopeo canal using *P. pulmonarius* and other bioremediation agents (bacteria and trees) was underway in Whakatane. (Thwaites, Farrell, Duncan, & White, 2007)

2.7 Summary

In conclusion, there is extensive research on PFAS and various removal technologies. Many studies have focused on eliminating PFAS from the environment or disposing of it, including from water sources. Several laboratory-scale experiments have used reactors to remove PFAS, while other research has explored the removal of short-chain PFAS from drinking water using granular activated carbon and biochar. This study will work towards combining biochar and fungi by attempting to grow fungi on biochar, to enable rapid adsorption of PFAS followed by slow degradation of PFAS by the fungi.

Chapter 3 – Methodology

3.1 Overview

The aim of this research was to evaluate biochar and fungi for the remediation of PFAS from water sources such as landfill leachate. The first part involved growing fungi on biochar and determining the optimal conditions for doing so, such as ideal moisture content, wood to biochar ratio, different types of substrate such as soil coir, mushroom spawn, wood compost, and fungi type. The second part involved measuring the adsorption properties of the biochar with humic acid and PFAS.

The experimental set-up was in C3.10 Environmental Engineering Laboratory in C Block at the University of Waikato, Hamilton, New Zealand. Analytical testing was performed mostly in C3.11 of the same building.

3.2 Reagents and chemicals

The following reagents and materials were used:

- Shitaki, oyster and pekipeki fungi (Mushroom by the Sea, Raglan)
- Mushroom spawn (Mushroom by the Sea, Raglan)
- Pine biochar (High BET) (Biogrow Ltd, Tauranga)
- Biochar (High grade) (Activated Carbon NZ Ltd, Taupo)
- Wood chip (Mitre 10, Hamilton)
- Soil coir (Mitre 10, Hamilton)
- Humic acid (Merck)
- Hydrogen peroxide (30%) (Merck)
- Potassium dichromate (Ajax)
- Chloroform (Merck)
- Potassium sulphate (Merck)
- Sucrose (Merck)
- Concentrated Sulphuric Acid (Merk)
- Distilled water (lab supply)
- Milli-Q (DI) water (lab supply)

- Aluminium sulphate (Merck)
- Piranha solution (33% hydrogen peroxide (30% strength), 67% concentrated sulfuric acid)
- Perfluoro heptanoic acid (Merck)
- Perfluoro hexanoic acid (Merck)
- Nonafluorobutane-1-sulphonic acid (Merck)

3.3 Equipment

3.3.1 Environmental Chamber

The fungi were grown in an 1.5 m by 0.6 m by 0.6 m environmental chamber made from acrylic (Laser Profiles, Hamilton), that was temperature-controlled to 24^{o}C using a Goldair bathroom wall mounted 2 kW fan heater (Mitre 10), controlled by a thermostat (made by the School of Engineering), and temperature and humidity were monitored using a Testo NZ portable sensor (Mitre 10).

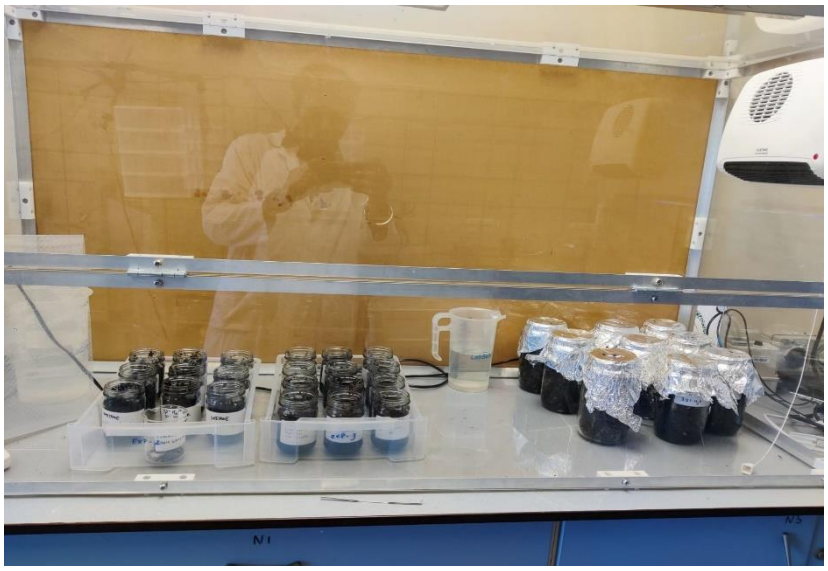

Figure 3-1 Environmental chamber with the exhaust fan for moisture control.

3.3.2 Arduino sensors

Duinotech Arduino compatible soil moisture sensors (Jaycar, Hamilton) and KS0049 Keyestudio soil humidity sensors coupled to an Arduino UNO board with a 12C 16x2 Arduino LCD display module (Figure 3-2) were used to measure the moisture content and the humidity content of the substrate used for growing the fungi. The Arduino UNO board was programmed using ArduinoCLI.

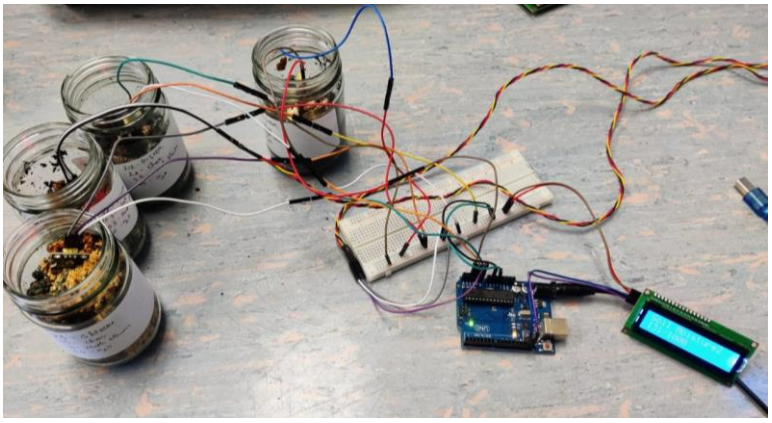

Figure 3-2 Arduino setup

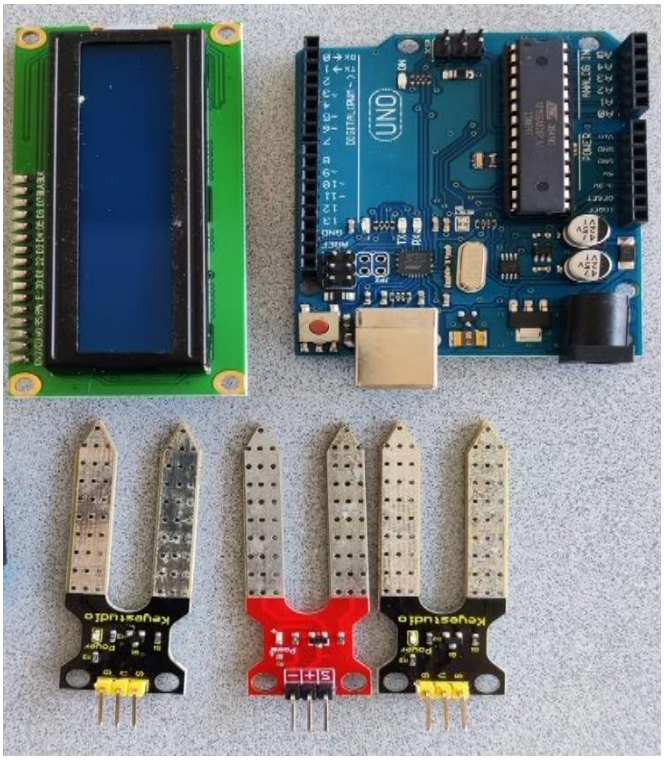

Figure 3-3 Arduino sensors and LCD display

The Arduno soil moisture sensors were calibrated using 20 g dry soil and 20 g dry biochar lots with 10, 20, 30, 40 and 50 g of water added. The substrate water mixtures were well mixed and left covered over the weekend at room temperature. The three Arduino probes were individually inserted into the moist substrate, the Arduino readings allowed to stablise and the final stable reading recorded (Figure XX). Actual substrate moisture contents were determined by taking samples of each substrate and oven drying overnight on a preweighed aluminium oven dish. Water content was calculated using the following equation:

Water content = Wet weight – Dry weight / Dry weight * 100

Arduino readings were plotted against substrate moisture content to produce a calibration curve.

Figure 3-4 Soil moisture reading

3.4 Fungi growth trials

Three different types of fungi (Shitaki, Oyster and Pekepeke) cultured on woodchip and mushroom spawn, as supplied by Mushroom by the Sea, were grown on different mixtures of substrate (biochar, woodchip, soil coir, wood compost, mushroom spawn) at different moisture contents and different starting culture concentrations. All cultures were grown in 250 ml glass jars (Science Stores) uncovered in the environmental chamber at 24 degrees C. Relative humidity was uncontrolled, but tended to be around 30%. Each trial is described below.

Trial 1 involved adding ~120 g of each culture to 50 g of biochar plus 80-90 g of water. Specific conditions are listed in Table 3.2. These cultures were grown for three weeks at room temperature, uncovered and open to the atmosphere. After three weeks, no growth was observed, the cultures had dried out, so an additional 50 g of water was added to each culture, and the cultures were left for another three weeks. No growth was observed so this trial was abandoned.

Table 33-1 Experimental conditions for trial 1 with biochar.

Fungi type	Culture(g)	Biochar(g)	Initial Water(g)	Total Weight(g)
Shiitake	120	50	85	255
Shiitake	125	50	90	265
Shiitake	120	50	80	250
Oyster	120	50	80	250
Oyster	120	50	80	250
Oyster	120	50	80	250
Pekepeke	120	50	80	250
Pekepeke	120	50	80	250
Pekepeke	120	50	80	250

Trial 2 involved adding 20 g of each culture to 20 g of biochar plus 70 g of water. These cultures were incubated for three weeks uncovered in the environmental chamber at 24^{o}C. Water content was too high, so no growth was observed and the trial was abandoned.

Table 3-2 Experimental conditions for trial 2 with biochar.

Fungi type	Culture(g)	Biochar(g)	Initial Water(g)	Total Weight(g)
Shiitake	20	20	70	110
Shiitake	20	20	70	110
Shiitake	20	20	70	110
Oyster	20	20	70	110
Oyster	20	20	70	110
Oyster	20	20	70	110
Pekepeke	20	20	70	110
Pekepeke	20	20	70	110
Pekepeke	20	20	70	110

Trial 3 involved using a combination of biochar and woodchip (Table 3), inncolulated with 15-20 g of fungal culture and incubating for three weeks.

Trial 4 used coco fiber soil coir as the primary medium, which expands when water is added. This coir was particularly effective for fungal growth, yielding impressive results in the cultivation of fungus. During the experiment, it was observed that the soil fiber block expands significantly upon the addition of water. To manage this, a smaller amount of soil fiber was used: 5 grams of soil fiber was mixed with 20 grams of biochar and 20 grams of mushroom substrate for each sample (Table 4).

Table 3-3 Experimental data for trial 3 with wood chip.

Fungi Type	Culture (g)	Biochar (g)	Woodchip (g)	Water (g)	Total weight (g)
Oyster 1	20	30	10	70	130
Oyster 1	20	20	15	70	125
Oyster 1	20	20	20	70	130
Oyster 2	20	20	20	70	130
Oyster 2	20	20	20	50	110
Oyster 2	20	20	25	50	115
Shiitake	20	20	20	50	110
Shiitake	20	20	15	50	105
Shiitake	15	20	15	50	100
Pekepeke	20	20	15	60	115
Pekepeke	15	20	20	60	115
Pekepeke	25	20	25	50	120

Figure 3-5 Coco fiber material

Figure 3-6 Soil coir mixed with biochar and shiitake mushroom

Table 3-4 Experimental data for trial 4 with soil coir.

Fungi type	Culture (g)	Biochar (g)	Soil Coir (g)	Water (g)	Total Weight (g)
Shiitake	10	20	5	70	105
Shiitake	20	20	5	60	105
Shiitake	15	10	5	70	100
Oyster	20	10	5	70	105
Oyster	20	15	5	70	110
Oyster	20	20	5	70	115
Pekepeke	20	20	5	70	115
Pekepeke	20	10	5	70	105
Pekepeke	10	15	5	80	110

Trial 5 used a combination of wood compost and biochar as the primary medium (Table 5). Trial 6 combined biochar with wood chip and soil coir with the following combinations (Table 6). Trial 7 used mushroom spawn with already cultivated mycelium on it.

Table 3-5 Experimental data for trail 5 with wood compost

Fungus type	Culture (g)	Biochar (g)	Wood compost (g)	Water (g)	Total weight (g)
Shiitake	20	20	20	70	130
Shiitake	20	15	15	70	120
shiitake	20	20	10	70	120
Oyster	20	20	10	70	120
Oyster	15	15	20	70	120
oyster	20	20	10	70	120
Pekepeke	20	20	10	70	120
Pekepeke	20	20	15	70	120
Pekepeke	20	10	10	70	110

Table 3-6 Trial 6 by mixing two component woodchip and soil coir with the new type of biochar (pine biochar)

Fungus Type	Culture (g)	Biochar (g)	Woodchip (g)	Soil coir (g)	Water (g)	Total weight (g)
Oyster	20	15	15	5	80	135
Oyster	20	15	20	5	80	140
Oyster	20	10	20	5	80	135
Shiitake	20	20	10	5	80	135
Shiitake	20	10	10	5	80	125
Shiitake	20	15	15	10	80	140
Pekepeke	20	10	5	5	90	130
Pekepeke	20	20	10	6	90	146
Pekepeke	20	15	10	10	90	145

Table 3-7 Trial 7 using mushroom spawn.

Fungus type	**Culture (g)**	**Biochar(g)**	**Mushroom spawn(g)**	**Water(g)**	**Total weight(g)**
Pekepeke	20	20	20	70	130
Pekepeke	20	15	10	70	115
Pekepeke	20	10	15	70	115
Shiitake	20	15	15	70	120
Shiitake	20	20	20	70	130
Shiitake	20	25	15	70	130
Oyster	20	20	15	70	125
Oyster	20	15	15	70	120
Oyster	20	10	20	70	120

3.5 Fungal growth measurement

Fungal growth was measured in three ways, the first using time lapse vision analysis, the second measuring biomass by extracting it using the reflux ratio method and the third was measuring biomass by incubating the samples in chloroform, extracting the biomass as sugars and measuring the quantity of sugars.

3.5.1 Time Lapse Fungal Growth

The primary objective of this experiment was to observe the initiation and progression of fungal growth, as well as to determine the number of days required for visible growth to occur. The process was captured using a Brinno time-lapse camera, which continuously recorded the growth over a 28-day period. The study specifically focused on comparing the rate of fungal

growth on woodchips and biochar to assess the relative speed of colonization on these substrates.

3.5.2 Reflux ratio method

The reflux ratio method involved dissolving fungal matter using alkali/methanol extraction by adding 2 grams of substrate containing fungi to 25 ml of methanol containing 2.5 mg of KOH into a 100 ml round bottom flask. A water-cooled condenser was attached to the top of the flask to condense the evaporated methanol and recycle it back into the flask. The flask was heated until the mixture was boiling and left to boil for 30 minutes. The mixture was left to cool for 2 hours after which 20 ml of methanol and 25 ml of n-hexane was added, and mixed thoroughly until a vortex was observed. This was left standing until the n-hexane had separated from the methanol. The n-hexane layer was decanted and filtered using 114 Whatman filter paper in a filter funnel, 10 ml of the liquid collected in a 10 ml plastic syringe and filtered again using a 0.45 μm syringe filter. Concentration of extract in n-hexane was measured by UV absorbance at 254 nm. This method was used for two samples, one containing 20 g of biochar and 70 g of water, from which 2 grams of the mixture was taken and analysed, the other from a mixture of 20 g each of oyster mushroom culture, biochar, woodchip and 70 g of water which had been left to incubate for three days.

Figure 3-7 Experimental setup for the reflux method for measuring fungal growth

3.5.3 Chloroform fumigation method

Six samples were analyzed for soluble organic carbon content using the chloroform fumigation method (Table 3-12).

Table 3-8 Analyzed organic carbon solution.

Sample	Oyster/ biochar	Shitake/ biochar	Oyster innoculum	Shitake innoculum	Biochar	Woodchip
Fungi type	Oyster	Shitake	Oyster	Shitake	None	None
Innoculum mass (g)	20	20	20	20		
Biochar mass (g)	20	20			20	
Woodchip (g)						20
Water (g)	70	70				
Total (g)	110	110	20	20	20	20
Water content (%)	64	64				
Culture time (days)	5	5	0	0	0	0

10 grams of each mixture were measured into beakers, and placed in a desiccator with 250 ml of chloroform, and left to fumigate for 15 days. After the 15-day fumigation period, 50 ml of 0.5M potassium sulfate (K_2SO_4) was added to each beaker to extract the soluble carbon content. 10 ml of each extract was filtered through a 0.45 um filter and 5 ml of each was added to a digestion tube along with 5 ml of 2.5M potassium dichromate ($K_2Cr_2O_7$), and 10 ml of concentrated H_2SO_4. 5 ml of 25 mg/L sucrose solution for a calibration standard and 5 ml of distilled water for the blank were also added to digestion tubes, and the digestion reagents were added to each. Afterward, all the tubes were heated for 30 minutes at 135 degrees Celsius in a Hach DRB 200 incubator, after which 55 ml of distilled water was added to each tube to make the volume up to 75 ml. The solutions were light red in colour, which was analysed at 600 nm in a UV/Vis spectrophotometer. Absorbance results were compared against the calibration standard to determine organic carbon content (mg/L at sucrose) in each of the extracts. Mass of organic carbon extracted was calculated by multiplying by the volume of extract solution added, and dividing by the mass of sample gave the organic carbon content per gram sample.

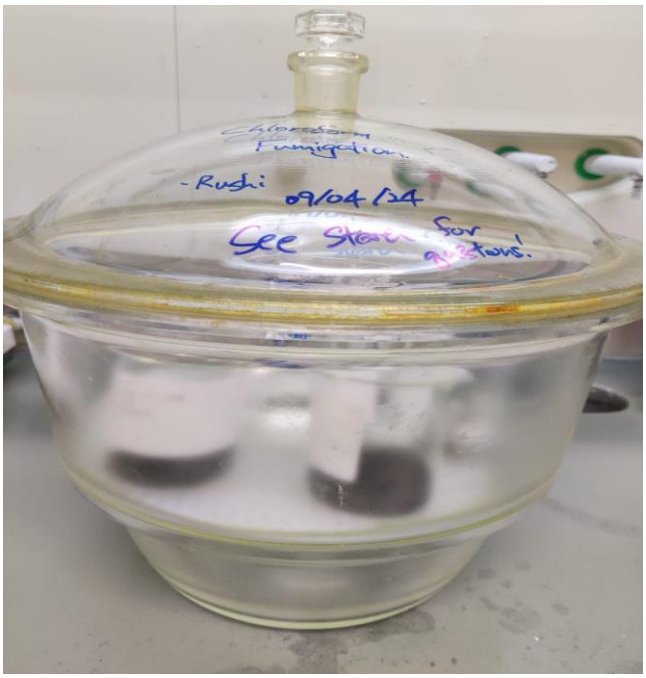

Figure 3-8 Mushroom fungus fumigated for 10 days with 250 ml chloroform

Figure 3-9 Incubation of samples for sugar analysis by digesting at 135 degrees Celsius.

3.6 Adsorption Isotherm Testing

A stock solution of 40 mg/L humic acid in distilled water was prepared in a 2 L volumetric flask. This was then diluted to 10, 20, and 30 mg/L, and 100 ml aliquots of each including distilled water and 40 mg/L solutions were added to conical flasks. Samples from each were used to measure UV absorbance at 254 nm in a Shimadzu UV/VIS spectrophotometer to prepare a calibration curve of UV absorbance versus humic acid concentration. 20 g of biochar was added to each conical flask and the solutions placed on a Ratek platform mixer overnight. Samples from each were collected and UV absorbance measured. An initial problem was found where the UV absorbance for the samples containing biochar was constant and did not correspond to the amount of humic acid added, so this trial was repeated, and repeated again with crushed and washed biochar, and then once more, this time with humic acid concentrations at 100, 200, 300 and 400 mg/L. The biochar was crushed using a Living & Co coffee and spice grinder and washed using distilled water.

Figure 3-10 Set up for adsorption isotherm testing.

3.7 Surface Charge Analysis

The surface charge of biochar was analysed using the Mutek PCD 03 particle charge detector. to investigate the interaction between biochar and humic acid. A stock solution of 1 g/L aluminium sulphate in distilled water was made. 1 g of ground biochar was mixed with 100 ml of distilled water, 10 ml of which was added to the particle charge detector and left to equilibrate. The initial charge was noted, and then 100 µL aliquots of alum solution was added, allowed to equilibrate, and the charge noted. This was repeated until the surface charge reached 0 mV.

3.8 PFAS Adsorption

Biochar was tested for its ability to adsorb three types of PFAS: perfluorobutanesulphonic acid (PFBSA), perfluorohexanoic acid (PFHexA), and perfluoroheptanoic acid (PFHepA).

To prevent cross contamination or accidental detection of PFAS, all glassware was cleaned with a solution made of 30% hydrogen peroxide and concentrated sulfuric acid in a 1:2 ratio and rinsed using milli-Q water.

Stock solutions of PFBSA, PFHexA and PFHepA was prepared by adding 10 mg of PFBSA to 100 ml of of ultrapure milli-Q water and 25 mg of PFHexA and PFHepA to 250 ml of ultrapure milli-Q water in volumetric flasks. These were diluted 1/10,000 by taking 10 µL of each stock solution, adding each to another 100 ml volumetric flask and filling these up with milli-Q water. The PFBSA was then diluted to 0, 25, 50, 75, and 100 ng/L concentrations, and the PFHexA and PFHepA was diluted to 0, 250, 500, 750, and 1000 ng/L, all in 100 ml volumetric flasks. These were transferred to 100 ml Shott bottles, 4 g of biochar was added to each, sealed, and these were left to equilibrate over two days in a dark room away from sunlight. All the samples were centrifuged at 4200 rpm in 50 ml Falcon tubes using a Sigma 6-15 centrifuge for 15 minutes. The samples were decanted into plastic sample bottles provided by Eurofins Food Analytics NZ Ltd and sent to Eurofins for PFAS analysis.

A 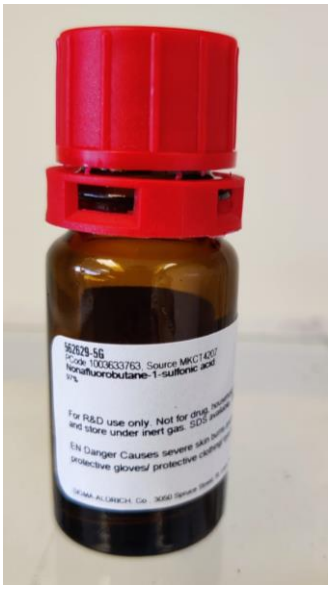 B 

Figure 3-11 PFAS –A) Perfluorobutanesulphonic acid, B) Perfluorohexanoic acid and perfluoroheptanoic acid

Figure 3-12 Sample preparation of all the PFAS

Table 3-9 Dates of the sample preparation of PFAS

Sample Name	PFAS species	Initial Conc (ng/L)	Prep date
Blank	None	0	05 September 2024
PFBSA25	Perfluorobutanesulfonic acid	25	02 September 2024
PFBSA50	Perfluorobutanesulfonic acid	50	02 September 2024
PFBSA75	Perfluorobutanesulfonic acid	75	02 September 2024
PFBSA100	Perfluorobutanesulfonic acid	100	02 September 2024
PFHexA250	Perfluorohexanoic acid	250	05 September 2024
PFHexA500	Perfluorohexanoic acid	500	05 September 2024
PFHexA750	Perfluorohexanoic acid	750	05 September 2024
PFHexA1000	Perfluorohexanoic acid	1000	05 September 2024
PFHepA250	Perfluoroheptanoic acid	250	05 September 2024
PFHepA500	Perfluoroheptanoic acid	500	05 September 2024

PFHepA750	Perfluoroheptanoic acid	750	05 September 2024
PFHepA1000	Perfluoroheptanoic acid	1000	05 September 2024

Figure 3-13 Centrifugation of PFAS sample

Chapter 4: Results and Discussions

In this chapter, the results from the soil moisture calibration, fungal growth trials, humic acid and PFAS adsorption and biochar surface charge analysis are presented and discussed.

4.1 Soil and biochar moisture calibration

Calibrating the Arduino soil moisture sensors showed that the sensors produced a linear result proportional to moisture content up to about 30% moisture content after which the readings plateaued (Figure 4-1). During the fungal growth trials, substrate moisture was kept around 60-70%, well outside the effective range of the Arduino moisture sensors, and all the Arduino readings were in the 600-1000 range. A soil moisture sensor that can measure up to 70% moisture content on a wet basis would be useful, but most moisture sensors are in the range of 30 to 50% moisture content.

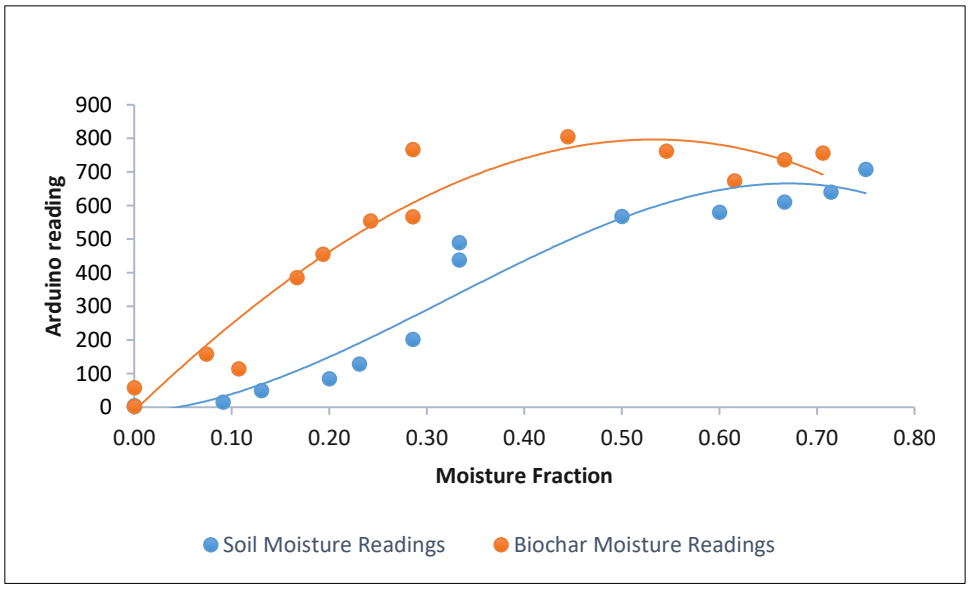

Figure 4-1 Comparison of soil and biochar moisture curve

4.2 Fungal growth trials

Out of all three types of fungi tested, oyster and shiitake mushroom gave the best growth, with oyster mushroom giving the best overall growth. Pekepeke showed little to no growth, and what did grow had a green colour which could have been algae or aspergillus fungi. Little or

no growth occurred on biochar itself (Trial 1 and Trial 2, Table 4-1, Figure 4-1), and if any growth did occur, it was on the material in the inoculum. This suggests that biochar is not very good at supporting growth, and is potentially inhibitory, particularly for pekepeke. Biochar can release polycyclic aromatic hydrocarbons which have a detrimental effect on cellular growth and microbiological activity and can be carcinogenic or mutagenic. Biochar with PAH greater than 300 mg/kg is not recommended for use in soil (Paulina Godlewska, 2021). Biochar is also rich in heavy metals which may also have an impact on fungal growth. Kavitha et al., (2018) and Sun et al., (2013), found biochar derived from corncob increased biomass of bacteria and fungi after addition to soil, while Han et al. (2016) found that biochar produced from pyrolyzed switchgrass (Panicum virgatum L.) at temperatures of 500 or 700 ◦C reduced mycorrhizal fungal growth in soil. Future work using biochar could examine the toxic compounds released from biochar and their effect on fungal growth and find production conditions and raw material sources that result in biochar with low PAH and heavy metals.

When woodchip was added, this greatly improved growth for oyster and shitaki mushroom giving the best overall results (Trial 3, Table 4-1, Figure 4-1). Moisture content appeared to have little effect on growth for Trial 3 within the moisture contents tried. This was different to Trial 1 and Trial 2 with biochar because in Trial 1 there was insufficient moisture (32%) and in Trial 2 there was potentially too much moisture for biochar (64%) where it was visibly wet. In the case of Trial 3, with moisture contents maintained between 50 to 70%, the woodchip absorbed most of the moisture because it is hydrophilic, whereas in Trial 1 and Trial 2, biochar has very little water holding capacity because it is hydrophobic because it was carbonized. Fungal growth was observed within just two days of initiating the experiment. The inclusion of woodchips created a more conducive environment for fungal growth, because oyster and shitaki mushrooms are primary decomposers of wood, preferring dead of dying wood, and is naturally found in temperate and subtropical forests on deciduous trees and beech trees (Roger

Phillips, 2006) (PM, 2004) Pekepeke favors dead trees or occupying the wounds in oak, maple, ash and eucalyptus trees (Swiecki, 2006).

Microscopic examination of the fungal growth of oyster mushroom and shitaki mushroom on woodchip from Trial 3 showed good evidence of mycelium growth and penetration (Figure 4.2, 4.3 and 4.4).

When soil coir was used as a substrate, shiitake mushroom showed quite impressive growth, and growth was better than when a combination of soil coir and wood chip was used. Whereas oyster mushroom favoured a combination of soil coir and wood better than soil coir alone. Soil coir is made from coconut husks, has an open pore structure increasing air penetration, water holding capacity (Growing Green nz, n.d.), and is probably easier for shitaki mushroom to populate compared to a combination of wood and soil coir, even though both shitaki and oyster gave much better growth when wood chip was added as substrate.

Wood compost as a substrate did not promote fungal growth, resulting in fourth best growth outcomes for both oyster and shitaki mushroom. This is possibly because it is a "finished" compost, primarily a humic material, with little substrate left for fungi to grow on (Diaz et al 2007, Compost Science and Technology). Composting typically consists of an initial rapid decomposition of easy to decompose compounds such as sugars, starches and proteins by bacteria at high temperatures reaching 70^{o}C over a period of two to four weeks, followed by a slow decomposition of cellulosic material by fungi at close to atmospheric temperatures over a period of months (Diaz et al 2007, Compost Science and Technology).

Mushroom spawn promoted the growth of oyster mushroom resulting the second-best growth for oyster mushrooms out of the seven trials, whereas it resulted in the worst growth for shitaki mushrooms out of all the trials that resulted in growth for shitaki mushrooms. This could be due to there being a better or fresher culture of oyster mushrooms on that particular variety of

mushroom compared the shitaki mushroom spawn and should be repeated with another batch of the mushroom to confirm.

4.3 Time Lapse Fungal Growth

Fungal growth for oyster and shitaki mushroom (20 g) on 20 g biochar, 5 g wood with the total mixture moisture content maintained at 70% water was monitored using a time lapse camera. Selected images were extracted and are shown in Table 4-3 and 4-1. The growth conditions were closest to Trial 2 from Table 4-3 and 4-1, but with 5 g wood chip added to help promote growth. Fungal growth for oyster mushroom was not obvious until day 5, which confirms results from Trial 2, while no growth was observed for shitaki at all. This was probably due to the moisture content and biochar content being too high and there not being enough woodchip to help absorb the water. Also, the innoculums used were old (about 7 months), so probably a better result would have been achieved with fresh inoculum. From day 10 to 12, it appears that aspergillus fungi (green colour) had started colonizing where the oyster mushroom was growing. We had hoped to use the image analysis to try to quantify fungal growth but the image quality was not good and fungal growth was less than expected. If this was to be repeated, it should be done using fresh inoculum, a greater wood content, and water content reduced to e.g. 60-65%, and with a better, high resolution camera, and reduce images captured to twice per day rather than every 30 minutes.

Trial	Fungi type	Repeat	Culture (g)	Biochar (g)	Woodchip (g)	Soil coir (g)	Wood compost (g)	Mushroom spawn (g)	Initial water (g)	Water content (%)	Growth ranking	Additional comments	Observations
1	Oyster	1	120	50					80	32	-	No moisture control	No growth, water content not high enough
1	Oyster	2	120	50					80	32	-		
1	Oyster	3	120	50					80	32	-		
2	Oyster	1	20	20					70	64	5	Some water added, probably too much	No visible growth up to day 5, some growth after 7 days. Composite sample from 1,2,3 used for chloroform fumigation experiment
2	Oyster	2	20	20					70	64	5		
2	Oyster	3	20	20					70	64	5		
3	Oyster	1	20	30	10				70	54	1-2	Maintained moisture at 70%	Best growth, out of all 7 trials, visible after 5 days. Water content amount had little or no visible impact on growth. 20 -25 g wood gave best oyster mushroom growth for this trial. Composite sample from 4,5,6 used for chloroform fumigation experiment
3	Oyster	2	20	20	15				70	56	1-2	Maintained moisture at 60%	
3	Oyster	3	20	20	20				70	54	1	Maintained moisture at 50%	
3	Oyster	4	20	20	20				70	54	1	Maintained moisture at 70%	
3	Oyster	5	20	20	20				50	45	1	Maintained moisture at 60%	
3	Oyster	6	20	20	25				50	43	1	Maintained moisture at 50%	
4	Oyster	1	20	10		5			70	67	3	Maintained moisture at 70%	Best growth, 3rd best out of all 7 trials
4	Oyster	2	20	15		5			70	64	3		
4	Oyster	3	20	20		5			70	61	3		
5	Oyster	1	20	20			10		70	58	4	Maintained moisture at 70%	Best growth, 4th best out of all 7 trials
5	Oyster	2	15	15			20		70	58	4		
5	Oyster	3	20	20			10		70	58	4		
6	Oyster	1	20	15	15	5			80	59	2	Maintained moisture at 80%, pine biochar	Pine biochar, best growth, 2nd best equal out of all 7 trials
6	Oyster	2	20	15	20	5			80	57	2		
6	Oyster	3	20	10	20	5			80	59	2		
7	Oyster	2	20	15				15	70	58	2	Maintained moisture at 70%	Best growth, 2nd best equal out of all 7 trials
7	Oyster	3	20	10				20	70	58	2		
7	Oyster	1	20	20				15	70	56	2		

Table 4-1 Experimental trial for fungal growth

Trial	Fungi type	Repeat	Culture (g)	Biochar (g)	Woodchip (g)	Soil coir (g)	Wood compost (g)	Mushroom spawn (g)	Initial water (g)	Water content (%)	Growth ranking	Additional comments	Observations
1	Pekepeke	1	120	50					80	32	-	No moisture control	No growth, water content not high enough
1	Pekepeke	2	120	50					80	32	-		
1	Pekepeke	3	120	50					80	32	-		
2	Pekepeke	1	20	20					70	64	-	Some water added, probably too much	No visible growth
2	Pekepeke	2	20	20					70	64	-		
2	Pekepeke	3	20	20					70	64	-		
3	Pekepeke	1	20	20	15				60	52	-	Maintained moisture at 70%	Some visible growth, no visible difference between trials 3, 5, 6 and 7, visible growth after 14 days, green colour, might be algae or another fungi, possibly Chlorociboria. Water content amount had little or no visible impact on growth
3	Pekepeke	2	15	20	20				60	52	-	Maintained moisture at 60%	
3	Pekepeke	3	25	20	25				50	42	-	Maintained moisture at 50%	
4	Pekepeke	1	20	20		5			70	61	-	Maintained moisture at 70%	No growth
4	Pekepeke	2	20	10		5			70	67	-		
4	Pekepeke	3	10	15		5			80	73	-		
5	Pekepeke	1	20	20			10		70	58	-	Maintained moisture at 70%	Some visible growth, no visible difference between trials 3, 5, 6 and 7, visible growth after 14 days, green colour, might be algae or another fungi, possibly Chlorociboria
5	Pekepeke	2	20	20			15		70	58	-		
5	Pekepeke	3	20	10			10		70	64	-		
6	Pekepeke	1	20	10	5	5			90	69	-	Maintained moisture at 80%, pine biochar	
6	Pekepeke	2	20	20	10	6			90	62	-		
6	Pekepeke	3	20	15	10	10			90	62	-		
7	Pekepeke	1	20	20				20	70	54	-	Maintained moisture at 70%	
7	Pekepeke	2	20	15				10	70	61	-		
7	Pekepeke	3	20	10				15	70	61	-		

Table 4-1 Experimental trial for fungal growth

Trial	Fungi type	Repeat	Culture (g)	Biochar (g)	Woodchip (g)	Soil coir (g)	Wood compost (g)	Mushroom spawn (g)	Initial water (g)	Water content (%)	Growth ranking	Additional comments	Observations
1	Shiitake	1	120	50					85	33	-	No moisture control	No growth, water content not high enough
1	Shiitake	2	125	50					90	34	-		
1	Shiitake	3	120	50					80	32	-		
2	Shiitake	1	20	20					70	64	6	Some water added, probably too much	No visible growth up to day 5, some growth after 7 days. Composite sample from 1,2,3 used for chloroform fumigation experiment
2	Shiitake	2	20	20					70	64	6		
2	Shiitake	3	20	20					70	64	6		
3	Shiitake	1	20	20	20				50	45	1	Maintained moisture at 70%	Good growth, best out of the 7 trials, visible after 5 days. Water content amount had little or no visible impact on growth
3	Shiitake	2	20	20	15				50	48	1	Maintained moisture at 60%	
3	Shiitake	3	15	20	15				50	50	1	Maintained moisture at 50%	
4	Shiitake	1	10	20		5			70	67	2	Maintained moisture at 70%	Good growth, 2nd best out of the 7 trials
4	Shiitake	2	20	20		5			60	57	2		
4	Shiitake	3	15	10		5			70	70	2		
5	Shiitake	1	20	20			20		70	54	4	Maintained moisture at 70%	Good growth, 4th best out of the 7 trials
5	Shiitake	2	20	15			15		70	58	4		
5	Shiitake	3	20	20			10		70	58	4		
6	Shiitake	1	20	20	10	5			80	59	3	Maintained moisture at 80%, pine biochar	Pine biochar, good growth, 3rd best out of the 7 trials
6	Shiitake	2	20	10	10	5			80	64	3		
6	Shiitake	3	20	15	15	10			80	57	3		
7	Shiitake	1	20	15				15	70	58	5	Maintained moisture at 70%	Good growth, 5th best out of the 7 trials
7	Shiitake	2	20	20				20	70	54	5		
7	Shiitake	3	20	25				15	70	54	5		

Table 4-1 Experimental trial for fungal growth

Trial	Oyster	Shitaki	Pekepeke
Trial 3 Wood chip after 7 days			
Trial 4 Soil coir after 7 days			
Trial 6 Woodchip and soil coir after 12 days			
Trial 7 Mushroom spawn after 7 days			

Table 4-2 Images of fungal growth on the biochar and other materials

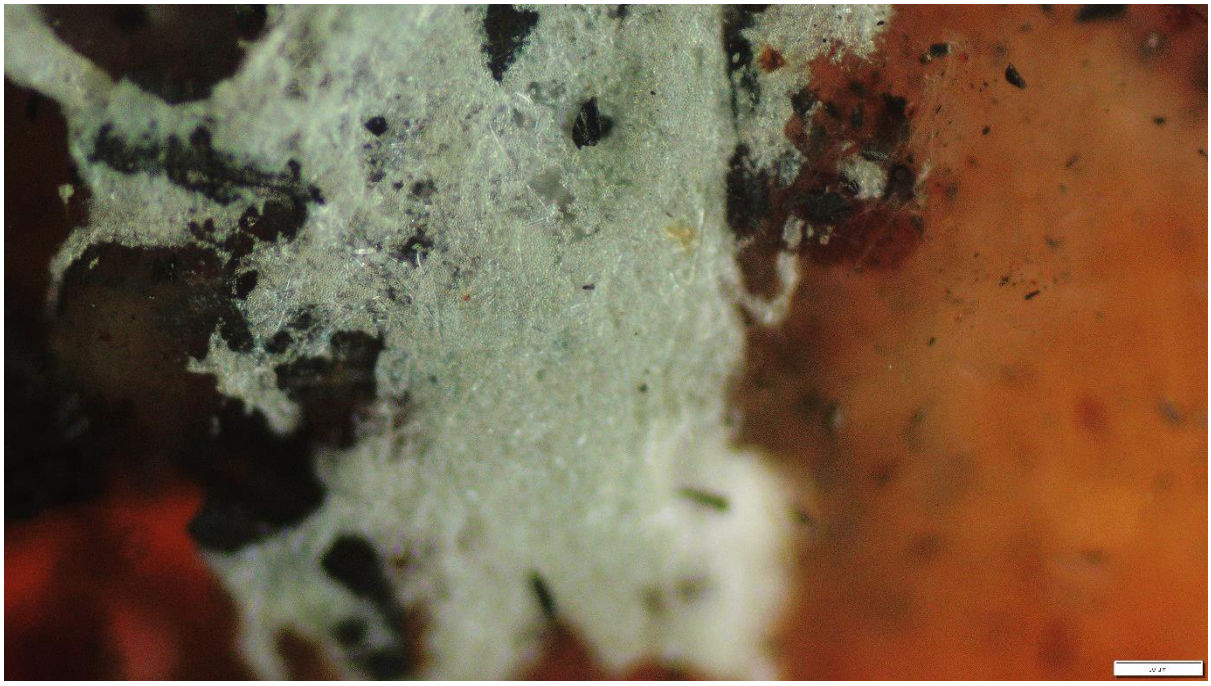

Figure 4-2. Microscope image of oyster fungal mycelia growing on the woodchip from Trial 3. Magnification 40x.

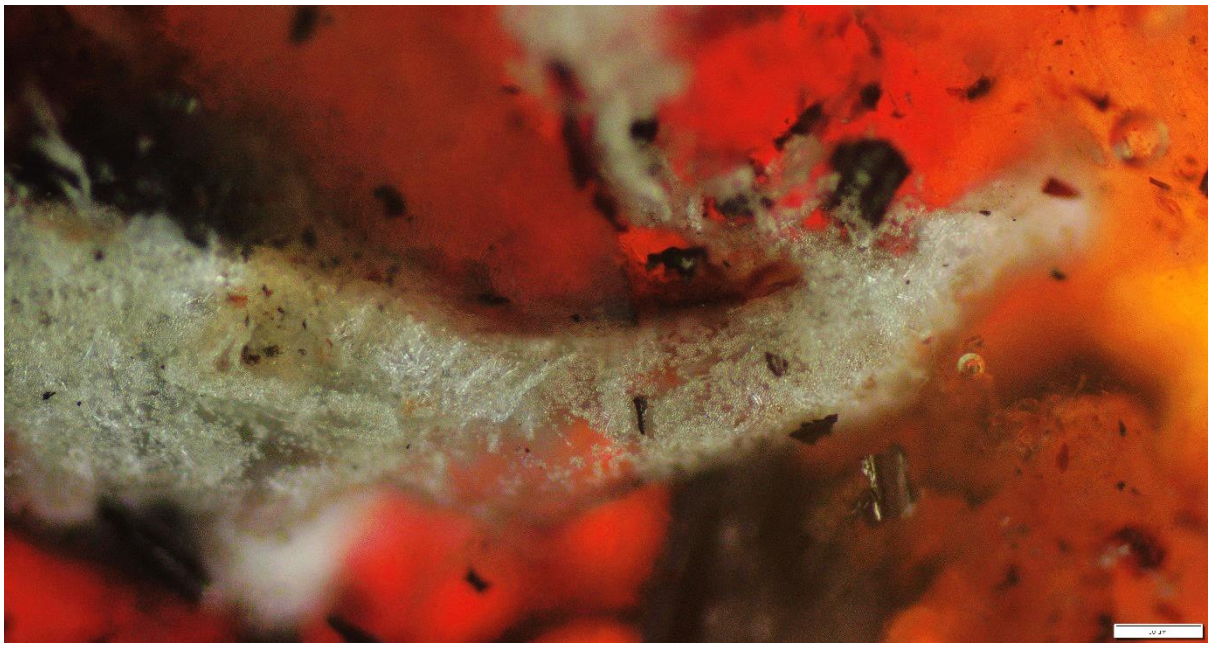

Figure 4-3 Microscope image of shiitake fungal mycelia growing on the woodchip from Trial 3. Magnification 40x.

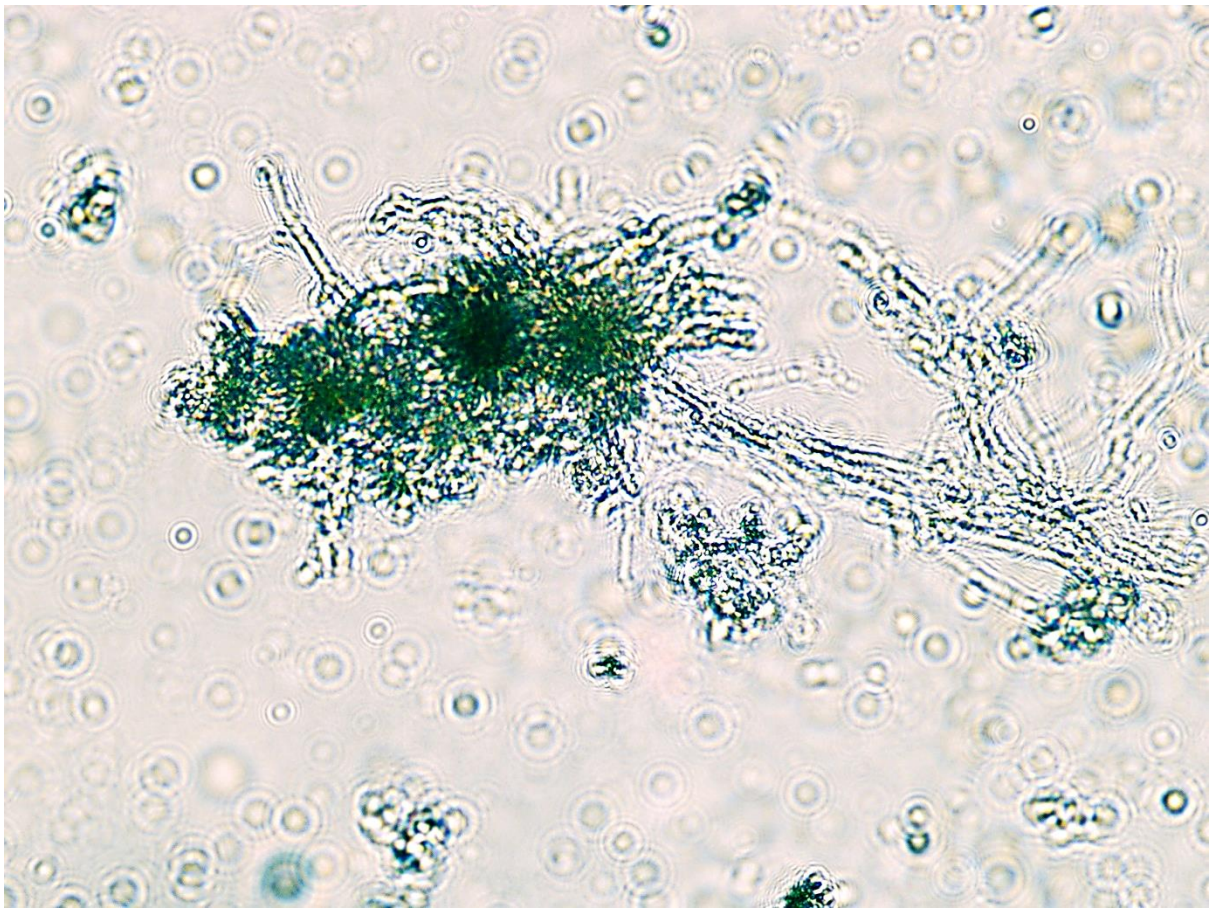

Figure 4-4 Microscope image of shiitake fungal mycelia growing on the woodchip from Trial 3 using phase contrast. Magnification 40x.

Table 4-3 Time lapse images of oyster and shiitake mushroom growth on woodchip and biochar

Day	Hour	Min	Video Capture

1	13	24	
4	9	0	
5	22	30	
8	3	22	
9	9	42	
10	19	37	

Table 4-3 Time-lapse images of oyster and shiitake mushroom growth on woodchip and biochar continued

Day	Hour	Min	Video Capture
11	20	57	
12	19	52	
13	12	0	
13	21	0	
14	2	2	

4.4 Measurement of fungal growth using the chloroform fumigation method

The chloroform fumigation method involves solubilizing the sugars present in the biomass by fumigating the samples with chloroform, followed by extracting the sugars using a salt solution, and then quantifying the sugars present using the reducing sugar assay. Fungal growth could be measured by a change in sugar content compared to what would be expected for starting conditions. Biochar and woodchip contain 5.7 and 37.2 mg/g sample of extractable sugars respectively (Table 4-4), while the starting oyster and shiitake inoculums have 127.7 and 228.1 mg/g extractable sugars. Using these numbers and the starting compositions for the oyster/biochar, shiitake/biochar and oyster/biochar/woodchip cultures, it was expected that the oyster/biochar would have an extractable sugar content of 24.2 mg/g, shiitake/biochar would have 42.4 mg/g and the oyster/biochar/woodchip would have 26.2 mg/g. After 5 days culture time, the sugar content in these three cultures were measured giving 112.4, 115.5 and 129.8 mg/g for oyster/biochar, shiitake/biochar and oyster/biochar/woodchip respectively. The difference between the expected and measured sugar concentrations was divided by the culture time to give an indication of culture growth. The oyster/biochar culture had a growth of 17.6 mg/g/day, while shiitake/biochar was 14.6 mg/g/day and the oyster/biochar/woodchip had a growth of 20.7 mg/g/day. This is comparable to Trial 2 where fungal growth was visible for the oyster and shiitake mushrooms on biochar after 5 days, and Trial 3 for oyster mushroom which had the best overall growth of all the trial conditions tried. Some papers use a correction factor as not all the sugars can be extracted from the sample after chloroform fumigation, with some using an extraction efficiency of around 50% (Yinjie Zhang, 2023), so potentially actual growth could be twice as much as what was reported in (Table 4-4). This method could be developed further by spiking control samples with e.g. a carbohydrate similar to what is in fungi cellular wall and testing extraction efficiencies. Fumigation times could be investigated as well, as in this study a fumigation time of 10 days was used, but some papers have used

much shorter fumigation times (Tranvik, 2003). The results from Table 4-4 were based on the averages from two repeats for each sample type, little variation was observed, but it could be worthwhile increasing the number of repeats. Also, it would also be useful to repeat the measurements for samples taken over multiple days to develop some growth trends.

Table 4-4 Fungal growth results using the chloroform fumigation method.

Parameters	Oyster/ biochar	Shiitake/ biochar	Oyster inoculum	Shiitake inoculum	Biochar	Woodchip	Oyster/ biochar/ woodchip
Fungi type	Oyster	Shiitake	Oyster	Shiitake	None	None	Oyster
Inoculum mass (g)	20	20	20	20			20
Biochar mass (g)	20	20			20		20
Woodchip (g)						20	20
Water (g)	70	70					70
Total (g)	110	110	20	20	20	20	130
Water content (%)	64	64					54
Culture time (days)	5	5	0	0	0	0	5
Organic content							
Innoculum mass (g)	2.55	4.56					2.55
Biochar mass (g)	0.11	0.11					0.11
Woodchip (g)							0.74
Total (g)	2.67	4.68					3.41
Expected (mg/g sample)	24.2	42.5					26.2
Measured (mg/g sample)	112.4	115.5	127.7	228.1	5.7	37.2	129.8
Growth (mg/g/day)	**17.6**	**14.6**					**20.7**

4.5 Reflux ratio method for measuring fungal growth

The reflux ratio method was successfully used to extract organic compounds from the culture used, resulting in a UV absorbance for extract in n-hexane of 600 mAu compared to the blank. However, this was not taken futher, mainly because of the process intensive steps to extract the organic compounds compared to the chloroform fumigation method. The reflux ratio involves extracting the sample over a hot plate and condensing and refluxing the n-hexane in an extraction hood. We only had provision for four of these apparatus at one time, while with the

chloroform fumigation method, as many samples could be extracted as could fit in the desiccator jars, and the sugar extraction just used potassium sulfate solution and did not require a volatile solvent and could be conducted in the lab. N-hexane is about 6 times more volatile than water (CHEMBL, n.d.) so care would be needed to avoid loss of solvent.

4.6 Humic Acid Adsorption

Calibration of the UV Spectrophotometer showed UV absorbance was proportional to humic acid concentration within the range tested (Figure 4-2).

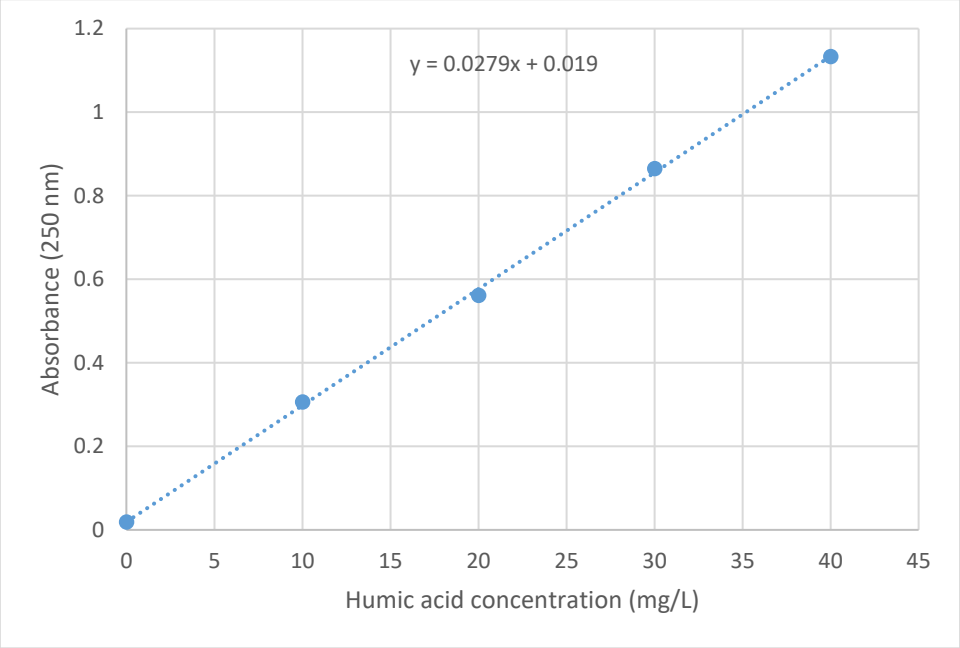

Figure 4-5 calibration curve sample test 1.

The first (Figure 4-2) and second (not shown) humic acid adsorption trial gave very similar results in that absorbance was constant (or at least flat) irrespective of starting humic acid concentration, and did not increase as expected as in when the humic acid does not adsorb on to the biochar. The first trial was assumed to be faulty and a second trial attempted but the same result was obtained. The blank (0 mg/L humic acid) showed significant organic matter coming off from the biochar elevating the UV absorbance readings, so when UV readings were baseline corrected to account for the organic matter coming off the biochar, it showed that all of the humic acid had adsorbed to the biochar. In the third trial the biochar was ground and washed prior to use to attempt to reduce the organic matter desorbing from the biochar. Starting humic acid concentration was also increased 10 fold. Once adsorption had taken place, humic acid readings in solution at equilibrium after baseline correction looked to be proportional to

starting humic acid concentration, and the majority of the humic acid had adsorbed to the biochar. The concentration on the biochar was obtained by subtracting the final humic acid concentration from the starting humic acid concentration, multiplying by the volume of solution and dividing by the mass of biochar. This was then plotted against the humic acid in solution at equilibrium to generate the isotherm. The Fruendlich, Langmuir and SIPS isotherms were fitted to the experimental data using Excel Solver to reduce the sum of square errors between the model data and experimental data (Table 4-5). There was little or no difference between the models, but based on the sum of square errors, the Fruendlich isotherm gave a slightly better fit. In the case of the SIPS model, because the K parameter was so low, the SIPS equation essentially reduced to the Fruendlich equation. The Langmuir equation suggested that the biochar had a low saturation capacity (Qmax) of close to 5 mg/g and that the biochar had a very low affinity (K) towards humic acid. Humic acid is a weak polyelectrolyte with pKa's ranging between 2.5 to 8.5 (Google search humic acid pKa), so at the pH used, not all of the charged groups on the humic acid would have been dissociated, i.e, they still retain the hydrogen ion so they would have a zero net charge. Biochar also has a range of charged groups, but for some biochar (e.g. that produced from tea), it does not reach a zero net charge until pH 2 (Ateş, 2023)

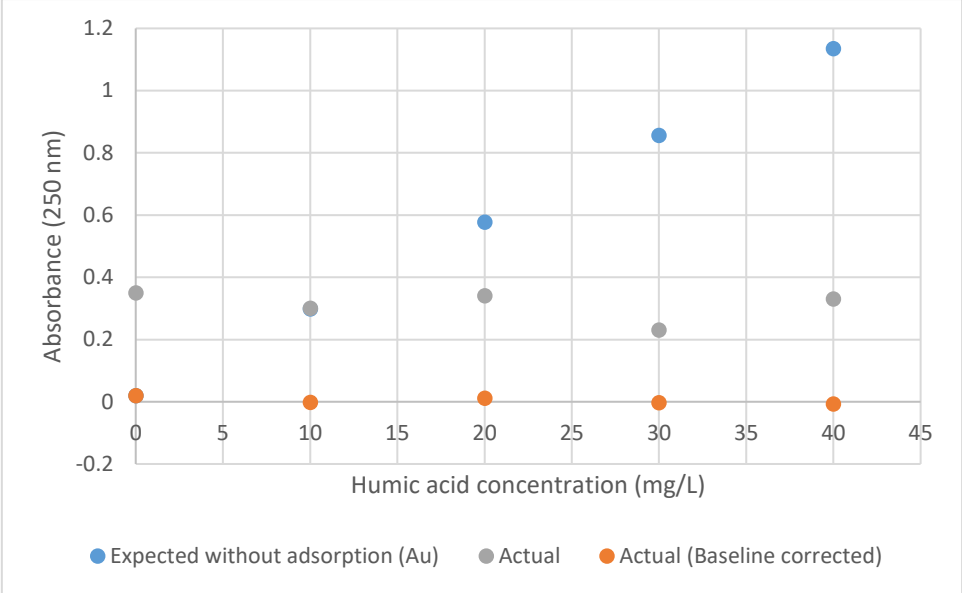

Figure 4-6 Humic acid expected absorbance and actual absorbance

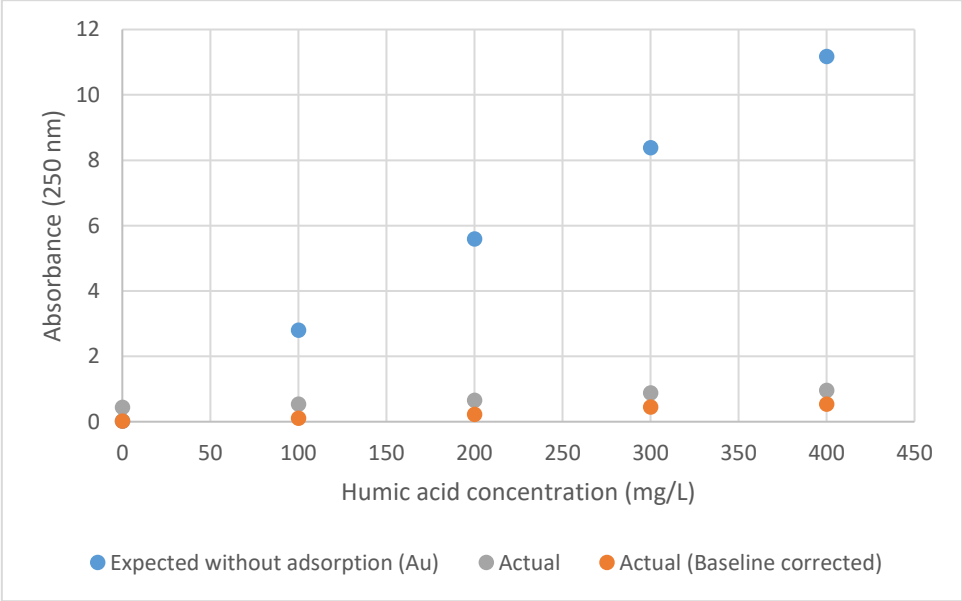

Figure 4-7 Humic acid adsorbance on biochar

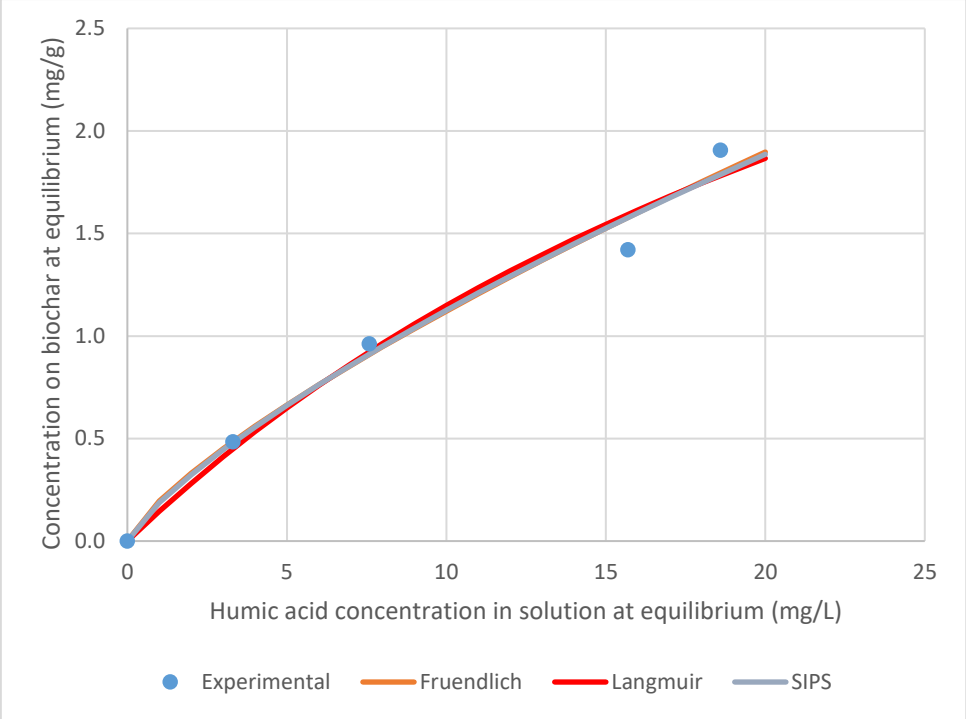

Figure 4-8 Humic acid isotherm calibration

Table 4-5 Isotherm Calculation

Parameter	Fruendlich	Langmuir	SIPS
K	0.196	0.030	0.008
Qmax (mg/g)		4.975	23.08
n (-)	0.758		0.796
SSE	0.040	0.048	0.041

Freundlich: $Q^* = KC^{*n}$

Langmuir: $Q^* = \frac{KC^*Q_{max}}{1+KC^*}$

SIPS: $Q^* = \frac{KC^{*n}Q_{max}}{1+KC^{*n}}$

Where Q^* and Q_{max} is the concentration (mg/g) on the biochar at equilibrium and saturation respectively, K is the equilibrium constant, C^* is the concentration in solution (mg/L) at equilibrium and n is a Freundlich or SIPS constant.

4.7 Surface Charge Analysis

Surface charge analysis of the biochar using the Mutek PCD showed that 3.66 ml of 1 g/L alum solution was needed to reduce the surface charge to zero for 0.04 g of biochar in 10 ml of water.

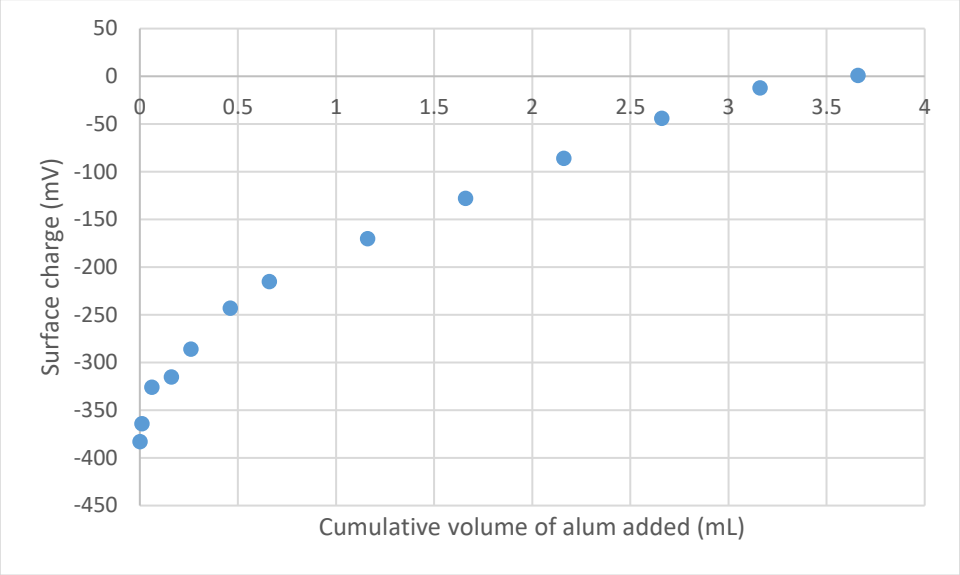

Figure 4-9 Adsorption curve for surface charge analysis

The mass of alum required was calculated by multiplying the volume of alum solution added by the concentration of alum in the solution. This was divided by the molecular weight of alum and the mass of biochar added to obtained mM Al^{3+} per gram biochar. This was then multiplied by the valency of the aluminium (3+) to obtain mM +ve ion added per g biochar which is also equal to the mM -ve charges per g biochar, which was 0.824 mM/g biochar. Dry soil has a surface charge of 0.125 mM/g soil, so the biochar used has about 6.6 times the amount of negative charges, which is not surprising given that biochar is mostly organic carbon with functional groups such as carboxyl groups whereas soil is largely silicate material with 10-20% organic content. Given the large number of negative charges on the biochar, it was not surprising that humic acid had a low affinity for biochar.

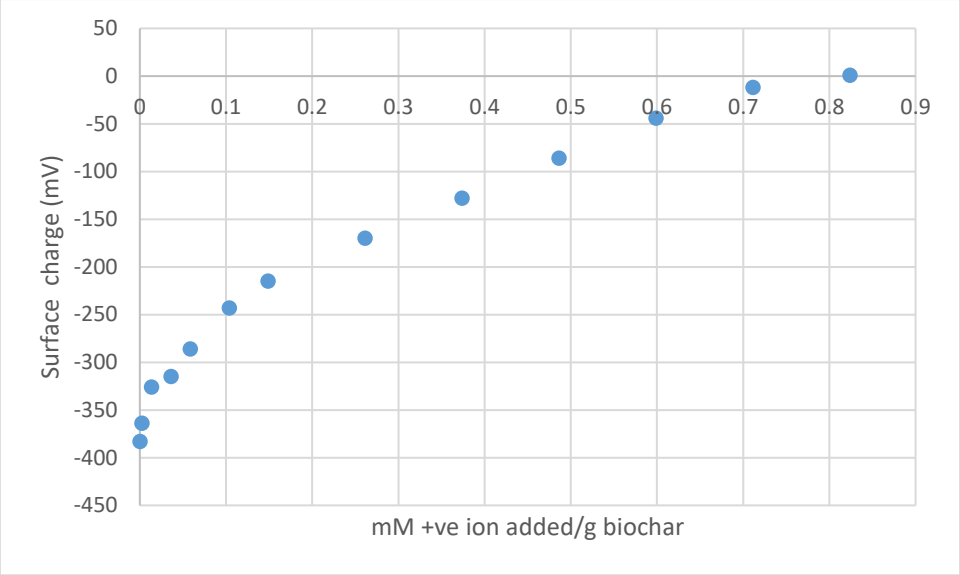

Figure 4-10 Surface charge of biochar vs mM +ve ions added.

4.8 PFAS adsorption

A total of 13 PFAS adsorption experiments on to biochar were conducted, including one blank. Starting concentrations were in the range that have reported to be found in the environment, typically in the 0-1000 ng/L range. The biochar used adsorbed all of the three types of PFAS tested, leaving concentrations of PFAS in solution below the detectable limit for tests conducted by Eurofins (Table 4-6). All the PFAS tested have a pka below -0.1 which means that the hydrogen ion on the carboxyl group or the sulfonic group (Figure 4-8) is dissociated and those groups have a negative charge. Biochar will also have an overall negative charge, but has a large number of functional groups on the surface that can act as hydrogen donors for hydrogen bonding. According to, (PubChem, n.d.) PFBSA can accept hydrogen bonds in 12 locations, while PFHexA and PFHepA can accept 13 and 15 hydrogen bonds respectively, therefore the PFAS adsorption to biochar will be predominantly by hydrogen bonding rather than electrostatic (Zhang et al 2023). Zhang et al (2023) have reported PFAS adsorption capacities for biochar in the range of 46 to 72 mg/g, whereas in the case of these experiments, the maximum concentration reached was 25 ng/g for the 100 ml 1000 ng/L PFHepA solution with 4 g biochar in it. Furthermore, we only had 25 mg each of PFHepA and PFHexA, so we

would have never reached PFAS saturation capacity for biochar, but could have achieved it with PFBSA of which we had a 5 g sample.

Table 4-6 Results for PFAS testing

PFAS	Starting concentration (ng/L)	Starting concentration (µg/L)	Final concentration (µg/L)
Blank	0	0	<0.01
PFBSA	25	0.025	<0.01
PFBSA	50	0.05	<0.01
PFBSA	75	0.075	<0.01
PFBSA	100	0.1	<0.01
PFHexA	250	0.25	<0.01
PFHexA	500	0.5	<0.01
PFHexA	750	0.75	<0.01
PFHexA	1000	1	<0.01
PFHepA	250	0.25	<0.01
PFHepA	500	0.5	<0.01
PFHepA	750	0.75	<0.01
PFHepA	1000	1	<0.01

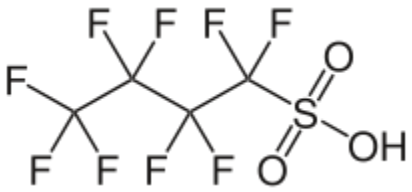

PFBSA pKa -3.1 (PubChem, n.d.)

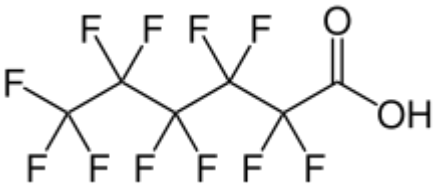

PFHexA pKa -0.16 (PubChem, n.d.)

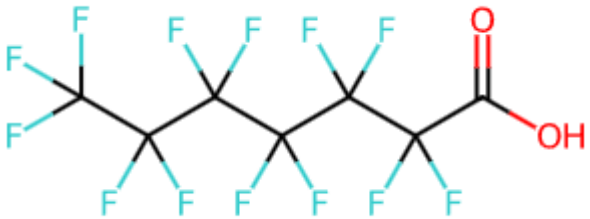

PFHepA pKa -2.29 (PubChem, n.d.)

Figure 4-11 Chemical structure of PFBSA, PFHexA, and PFHepA. (PubChem, n.d.)

Chapter 5: Conclusions and Recommendations

This research involved working towards developing a coupled system for PFAS treatment which involved using biochar for rapid capture and fungi populating the biochar to degrade the PFAS. The work was broken into several stages, the first finding suitable growing conditions for fungi on biochar and attempting to quantify the growth, the second examining biochar adsorption properties, first with humic acid and the second with PFAS.

Out of all three types of fungi tested, oyster and shiitake mushroom gave the best growth, with oyster mushroom giving the best overall growth. Pekepeke showed little to no growth, and what did grow had a green colour which could have been aspergillus fungi. Best growing conditions were a combination of woodchip and biochar. Biochar as a substrate by itself was not as conducive to growth, with oyster and shiitake mushroom taking up to five days to show signs of growth. Soil coir promoted the growth of shitaki mushroom while oyster mushroom preferred a combination of woodchip and soil coir. Wood compost was not conducive to growth, presumably because there was little left for the fungi to grow on.

Using soil moisture probes to monitor substrate moisture was not successful as they were only suitable for soil moisture content between 0-30% on a wet basis.

The chloroform fumigation method was the best for quantifying fungal growth, it was easy to implement, multiple samples could be done at the same time, and relied on being able to extract and quantify sugars from the fumigated samples. This method showed that the oyster/biochar culture had a growth of 17.6 mg/g/day, while shiitake/biochar was 14.6 mg/g/day and the oyster/biochar/woodchip had a growth of 20.7 mg/g/day.

Biochar had a low adsorption capacity and affinity for humic acid. The Langmuir equation suggested that the biochar had a low saturation capacity of close to 5 mg/g and that equilibrium constant was 0.03. The Freundlich isotherm gave a marginally better fit than the Langmuir and

SIPS isotherms. The low adsorption was due to both humic acid and biochar having predominantly negative charges, supported by surface charge analysis of the biochar using the Mutek particle charge detector which showed biochar had a surface charge of 0.824 mM -ve charges/g biochar, six times that of dry soil which has a surface charge of 0.125 mM/g soil.

Biochar was tested for its ability to adsorb three species of PFAS (PFBSA, PFHexA, PHHepA). Under the environmentally relevant PFAS concentration ranges tested, biochar adsorbed all of the PFAS, resulting in no PFAS being able to be detected in solution. While both biochar and PFAS are negatively charged, biochar has a large number of functional groups on the surface, that act as hydrogen bond donors while PFAS has a large number of hydrogen bond acceptors, therefore PFAS adsorption to the biochar is predominantly by hydrogen bonding rather than electrostatic.

For future work, the following recommendations are suggested:

For soil moisture monitoring, a soil moisture sensor that can measure up to 70% moisture content on a wet basis would be useful, but most moisture sensors are in the range of 30 to 50% moisture content.

Biochar can release polycyclic aromatic hydrocarbons which have a detrimental effect on cellular growth and microbiological activity and can be carcinogenic or mutagenic. Biochar can also be rich in heavy metals which may also have an impact on fungal growth. Future work using biochar could examine the toxic compounds released from biochar and their effect on fungal growth and find production conditions and raw material sources that result in biochar with low PAH and heavy metals.

Care needs to be taken with the age of fungi in the innoculums used, some trials e.g. for time lapse analysis were affected by the inoculum being old, resulting in slow or no growth.

For the chloroform fumigation method for measuring fungal growth, some papers use a correction factor as not all the sugars can be extracted from the sample after chloroform fumigation. This method could be developed further by spiking control samples with a carbohydrate similar to what is in the fungi cellular wall and testing extraction efficiencies. Fumigation times could be investigated as well and it would also be useful to repeat the measurements for samples taken over multiple days to develop some growth trends.

Time lapse analysis of fungal growth requires a high-resolution camera and image capture could be reduced to twice per day rather than every 30 minutes.

The saturation capacity of biochar for PFAS was not reached, so future work would need to use much higher starting PFAS concentration, or set up the biochar in some filter column where fresh solution is continuously applied to the biochar until PFAS is detected in the effluent.

Future work would need to examine the effect of fungi remediation on PFAS by different species of fungi itself, in tandem with adsorption onto biochar populated with fungi, or where the fungi is applied to the biochar after PFAS has been adsorbed to biochar.

References

(n.d.).

(n.d.). Retrieved from Growing Green nz: https://www.growinggreen.nz/

Amstaetter, K., Eek, E., & Cornelissen, G. (2012, April). Sorption of PAHs and PCBs to activated carbon: Coal versus biomass-based quality. *Chemosphere*, 6. Retrieved from https://doi.org/10.1016/j.chemosphere.2012.01.007

Arfin, T., Bushra, R., & Mohammad, F. (2016, December). Electrochemical sensor for the sensitive detection of o-nitrophenol using graphene oxide-poly(ethyleneimine) dendrimer-modified glassy carbon electrode. 10. Retrieved from https://link.springer.com/article/10.1007/s41127-016-0002-1

Ateş, A. (2023). The efect of microwave and ultrasound activation. *Biomass Conversion and Biorefnery*, 20. Retrieved from Biomass Conversion and Biorefnery (2023) 13:9075–9094

Belkouteb, N., Franke, V., McCleaf , P., Kohler, S., & Ahrens, L. (2020, September 1). Removal of per- and polyfluoroalkyl substances (PFASs) in a full-scale drinking water treatment plant: Long-term performance of granular activated carbon (GAC) and influence of flow-rate. *Water Research*, 10. Retrieved from https://doi.org/10.1016/j.watres.2020.115913

Bonato, M., Corrà, F., Bellio, M., Guidolin, L., Tallandini, L., Irato, P., & Santovito, G. (2020, October 30). PFAS Environmental Pollution and Antioxidant Responses: An Overview of the Impact on Human Field. *International Jounal of Environmental Research and Public Health*, 45. doi:https://doi.org/10.3390/ijerph17218020

Butt, T., Gouda, H., & Baloch, M. (2014, February). Literature review of baseline study for risk analysis — The landfill leachate case. *Environment International*, 14. Retrieved from https://doi.org/10.1016/j.envint.2013.09.015

Cerlanek, A., Liu, Y., Robey, n., Timshina, A. S., Bowden, J. A., & Townsend, T. G. (2024, February 15). Assessing construction and demolition wood-derived biochar for in-situ per- and polyfluoroalkyl substance (PFAS) removal from landfill leachate. *Waste Management*, 382-389. Retrieved from https://doi.org/10.1016/j.wasman.2023.12.017

CHEMBL. (n.d.). *wikiepedia*. Retrieved from https://en.wikipedia.org/wiki/Hexane#References

Dalahmeh, S. S., Alziq, N., & Ahrens , L. (2019, April). Potential of biochar filters for onsite wastewater treatment: Effects of active and inactive biofilms on adsorption of per- and polyfluoroalkyl substances in laboratory column experiments. *Environmental Pollution*, 10. Retrieved from https://doi.org/10.1016/j.envpol.2019.01.032

Douna, B. K., & Yousefi, H. (2023, Mar 2). Removal of PFAS by Biological Methods. *Asian Pacific Journal of Environment and Cancer*, 12. doi:10.31557/apjec.2023.6.1.53-68

Downie. (2009). Physical Properties of Biochar. In A. Downie, A. Crosky, & P. Munroe, *Biochar for Environmental Management* (p. 20). Taylor and Francis Group.

Du, Z., dang, s., Chen, Y., Wang, B., Huang, J., Wang, Y., & Yu, G. (2015, April 9). Removal of perfluorinated carboxylates from washing wastewater of perfluorooctanesulfonyl fluoride using activated carbons and resins. *Journal of Hazardous Materials*, 8. Retrieved from https://doi.org/10.1016/j.jhazmat.2014.12.037

Emiliano, e. (2022, January 18). PFAS Molecules: A Major Concern for the Human Health and the Environment. 55. doi:10.3390/toxics10020044

Gadzhiev, N., Vagapova, A., & Elmurzaev, R. (November 2023). Methods for monitoring greenhouse gases on the example of the mountain landscapes of the Chechen Republic. 10. Retrieved from 10.1051/bioconf/20237609005

Gaines Linda G.T, G. S. (2023, January 11). A proposed approach to defining per- and polyfluoroalkyl substances (PFAS) based on molecular structure and formula. *Intigrated Environmental Assessment and management*, 15. doi:10.1002/ieam.4735

Jay., M., Brouno, d. S., Kewalramani, J. A., & Casarini, M. M. (2022). A review of PFAS Destruction Technologies. doi:https://doi.org/10.3390/ijerph192416397

Keenan, J. D., Steiner, R., & Fungaroli, A. (1984, January). Landfill Leachate Treatment. *Water Pollution Control Federation*, 33. Retrieved from https://www.jstor.org/stable/25042153

Laura, C. M. (2023). National Survey of Pesticides In Groundwater 2022. 37. Retrieved from https://www.knowledgeauckland.org.nz/media/m1ncztyh/national-survey-pesticides-in-groundwater-2022-esr-june-2023.pdf

Li, X., Yang, Z., Wang, P., Yan, Y., & Ran, J. (2020). *Adsorption materials for volatile organic compounds (VOCs) and the key factors for VOCs adsorption process: A review*. Retrieved from https://doi.org/10.1016/j.seppur.2019.116213

Liu, N., Wu, C., Lyu, G., & Li, M. (2021, December 1). Efficient adsorptive removal of short-chain perfluoroalkyl acids using reed straw-derived biochar (RESCA). *Sceince of the Total Environmental*, 10. Retrieved from https://doi.org/10.1016/j.scitotenv.2021.149191

Meegoda Jay N., D. s. (2022). A Review Of PFAS Destruction Technologies. 25. doi: https://doi.org/10.3390/ijerph192416397

Militao, I. M., Roddick, F., & Fan, L. (2023, July). PFAS removal from water by adsorption with alginate-encapsulated plant albumin and rice straw-derived biochar. *Journal of Water Process Engineering*, 11. Retrieved from https://doi.org/10.1016/j.jwpe.2023.103616

Mohobane, T. (2008). The Characteristics and Impacts of Landfill Leachate from Horotiu, New Zealand and Maseru, Lesotho: A Comparative Study. Retrieved from https://hdl.handle.net/10289/2421

Mrabet, I. E., Benzina, M., & Valdés, H. (2020, July). Treatment of landfill leachates from Fez city (Morocco) using a sequence of aerobic and Fenton processes. *Scientific African*, 9. Retrieved from https://doi.org/10.1016/j.sciaf.2020.e00434

Occurrence, Fate, and Related Health Risks of PFAS in Raw and Produced Drinking Water. (2023, February 13). *Contaminants in Aquatic and Terrestrial Environments*, 13.

Paulina Godlewska, Y. S. (2021). THE DARK SIDE OF BLACK GOLD: Ecotoxicological aspects of biochar and biochar-amended soils. (D. C. tsang, Ed.) *Hazardous Materials*, 21.

PM, B. M. (2004). *Encyclopedia Of Diatery Supplements.* Retrieved from https://books.google.com/books?hl=en&lr=&id=WoW1DwAAQBAJ&oi=fnd&pg=PR14&dq=Encyclopedia+of+Dietary+Supplements&ots=oumcV1LMgy&sig=iark9HyuG5aYfETjnOM8uTwd3v8

PubChem. (n.d.). Retrieved from National library of medicine: https://pubchem.ncbi.nlm.nih.gov/compound/Perfluorobutanesulfonic-acid

Roger Phillips, D. A. (2006). *Mushrooms.* doi:ISBN 9780330442374

Sadia Mohammad, N. I. (2023). Occurrence, Fate, and Related Health Risks of PFAS in Raw and Produced Drinking Water. 54. doi:https://doi.org/10.1021/acs.est.2c06015

Shahsavari Esmaeil, R. D. (2021). Challenges abd Current Status of the Biological Treatment Of PFAS Contaminated Soils. 15. doi:https://doi.org/10.3389/fbioe.2020.602040

Silvani, L., Cornelissen, G., Smebye, A. B., Zhang, Y., Okkenhaug, G., Zimmerman , A. R., . . . Hale, S. E. (2019, December 1). Can biochar and designer biochar be used to remediate per- and polyfluorinated alkyl substances (PFAS) and lead and antimony contaminated soils? *Science of The Total Environment*, 9. Retrieved from https://doi.org/10.1016/j.scitotenv.2019.133693

Sinclair Georgia M., S. M. (2020). What are the effects of PFAS exposure at environmentally relevant. *Chemosphere*, 15. doi:https://doi.org/10.1016/j.chemosphere.2020.127340'

Singh, R. K., Brown, E., Thagard, S. M., & Holsen, T. M. (2021, April 15). Treatment of PFAS-containing landfill leachate using an enhanced contact plasma reactor. *Journal of Hazardous Materials*, 7. Retrieved from https://doi.org/10.1016/j.jhazmat.2020.124452

Swiecki, T. J. (2006). A Field Guide To Insects and diseases of california oaks. *Technical Report*, 158. doi: https://doi.org/10.2737/PSW-GTR-197

Tan, X., Liu, Y., Zeng, G., Wang, X., Hu, X., & Gu, Y. (2015). *Application of biochar for the removal of pollutants from aqueous solutions.* doi:https://doi.org/10.1016/j.chemosphere.2014.12.058

Thwaites, J., Farrell, R., Duncan, S., & White, R. (2007). *Fungal-Based Remediation: Treatment of PCP Contaminated Soil in New Zealand.* doi:https://doi.org/10.1007/978-3-540-34793-4_20

Tranvik, C. M.-L. (2003). Antagonism between Bacteria and Fungi on Decomposing Aquatic Plant Litter. 182. Retrieved from http://www.jstor.com/stable/4287692

Uriakhil, M. A., Sidnell, T., Fernández, A. D., Lee, J., Ross, I., & Bussemaker, M. (2021, November). Per- and poly-fluoroalkyl substance remediation from soil and sorbents: A. *Chemosphere*, 18. Retrieved from https://doi.org/10.1016/j.chemosphere.2021.131025

Uriakhil, M. A., Sidnell, T., Fernández, A. D., Lee, J., Ross, I., & Bussemaker, M. (2021, November). Per- and poly-fluoroalkyl substance remediation from soil and sorbents: A review of adsorption behaviour and ultrasonic treatment. *Chemosphere*, 18. Retrieved from https://doi.org/10.1016/j.chemosphere.2021.131025

Wang, F., Lu, X., Shih, K. M., Wang, P., & Li, X. (2014, 10 December). Removal of perfluoroalkyl sulfonates (PFAS) from aqueous solution using permanently confined micelle arrays (PCMAs). *Separation and Purification Technology*, 6. Retrieved from https://doi.org/10.1016/j.seppur.2014.09.037

Weber, K., & Quicker, P. (2018, April 1). Properties of biochar. *Fuel*, 22. Retrieved from https://doi.org/10.1016/j.fuel.2017.12.054

Xiang, W., Zhang, X., & Chen, J. (2020, August). Biochar technology in wastewater treatment: A critical review. *Chemosphere*, 14. Retrieved from https://doi.org/10.1016/j.chemosphere.2020.126539

Yinjie Zhang, X. T. (2023). Enhanced Removal of Polyfluoroalkyl Substances by Simple Modified Biochar; Adsorption Performance and Theoretical Calculation. *ACS Es&T Water*, 10. doi:10.1021/acsestwater.2c00597

Zang yinjie, T. X. (2023). Enhanced Removal of Polyfluoroalkyl Substances by Simple Modified Biochar: Adsorption Performance and Theoretical Calculation. 10. Retrieved from https://pubs.acs.org/doi/10.1021/acsestwater.2c00597?ref=pdf

Zareitalabad, P., Siemens, J., Hamer, M., & Amelung, W. (2013, May). Perfluorooctanoic acid (PFOA) and perfluorooctanesulfonic acid (PFOS) in surface waters, sediments, soils and wastewater – A review on concentrations and distribution coefficients. *Chemosphere*, 8. Retrieved from https://doi.org/10.1016/j.chemosphere.2013.02.024

Zhang, J., Pang, H., Gray, S., Ma, S., Xie, Z., & Gao, L. (2021, August). PFAS removal from wastewater by in-situ formed ferric nanoparticles: Solid phase loading and removal efficiency. *Journal of Environmental Chemical Engineering*, 10. Retrieved from https://doi.org/10.1016/j.jece.2021.105452

Zhi, Y., & Liu, J. (2015, July). Adsorption of perfluoroalkyl acids by carbonaceous adsorbents: Effect of carbon surface chemistry. *Environmental Pollution*, 9. Retrieved from https://doi.org/10.1016/j.envpol.2015.03.019

de Bruecker, T. (2015). Status report PFOS remediation. DEC Environ. Solutions 12. D'eon, J. C., and Mabury, S. A. (2007). Production of perfluorinated carboxylic acids (PFCAs) from the biotransformation of polyfluoroalkyl phosphate surfactants (PAPS): exploring routes of human contamination. Environ. Sci. Technol. 41, 4799–4805. doi: 10.1021/es070126x

Presentato, A., Lampis, S., Vantini, A., Manea, F., Dapr,à, F., Zuccoli, S., et al. (2020). On the Ability of perfluorohexane sulfonate (PFHxS) bioaccumulation by two Pseudomonas sp. strains isolated from PFAS-contaminated environmental matrices. Microorganisms 8:92. doi: 10.3390/microorganisms801009

Appendix

A.1 Fumigation Method measurements

Table A-1 Data for the fumigation method

	Concentration (M)	**Concentration (mg/L)**	**Total volume (ml)**	
K2SO4 solution	0.5		250	
K2Cr2O7	2.5		500	
H2SO4	18.4			
Sucrose		25	25	
	Oyster mushroom growing on biochar	**Shiitake mushroom growing on biochar**	**Sucrose**	**Blank**
Sample	F1	F2		
mass (g)	10	10		
Fumigation with chloroform				
Extraction with K_2SO_4 (ml)	50	50		
Syringe filter				
Filtrate volume (ml)	10	10		
Digestion				
Filtrate volume (ml)	5	5	2.5	2.5
K2Cr2O7 solution (ml)	5	5	2.5	2.5
H2SO4 solution (ml)	10	10	5	5
Distilled water (ml)	55	55	15	27.5
Total volume (ml)	75	75	25	37.5
Dilution	1	1	1.5	1
UV reading 1 (600 nm)	0.1436	0.1461	0.0531	0.0078
UV reading 2 (600 nm)	0.1435	0.1485		

Table A-2 Data for fumigation metho test 2

	Oyster inoculum	**Shiitake inoculum**	**Biochar**	**Woodchip**	**Oyster mushroom growing on woodchip and biochar**	**Blank**
mass (g)	10	10	10	10	10	
extraction with K2SO4 (ml)	50	50	50	50	50	
Filtrate volume (ml)	10	10	10	10	10	
Digestion	5	5	5	5	5	2.5
Filtrate volume (ml)	5	5	5	5	5	2.5
K2Cr2O7 solution (ml)	10	10	10	10	10	5
H2SO4 solution (ml)	55	55	55	55	55	27.5
Distilled water (ml)	75	75	75	75	75	37.5
Dilution	1	1	1	1	1	1
UV reading 1 (600 nm)	0.1762	0.2981	0.0287	0.0672	0.1788	0.0219
UV reading 2 (600 nm)	0.1765	0.2972	0.0292	0.0669	0.179	0.0223

Table A-3 Average carbon concentration media

	Oyster mushroom growing on biochar	**Shiitake mushroom growing on biochar**	**Sucrose**	**Blank**	**Oyster Inoculum**	**Shiitake Inoculum**	**Biochar**	**Woodchip**
Average reading corrected for blank	0.13575	0.1395	0.0453	0	0.15425	0.27555	0.00685	0.04495
Average reading corrected for dilution	0.13575	0.1395	0.0302	0	0.15425	0.27555	0.00685	0.04495
Organic carbon concentration (as sucrose) (mg/L)	112.4	115.5	25		127.7	228.1	5.7	37.2
Total organic carbon (as sucrose) (mg)	1123.8	1154.8			1276.9	2281.0	56.7	372.1
Organic carbon concentration in media (as sucrose) (mg/g)	112.4	115.5			127.7	228.1	5.7	37.2

Table A-4 Chloroform Fumigation Curve trial

Chloroform Fumigation Method Curve

Test 1

Oyster	Shiitake	Char	Woodchip	Sucrose	Experiment 1	Blank
0.1436	0.1461			0.0531		0.0078
0.1435	0.1485			0.0434		0.0089

Test 2

Oyster	Shiitake	Char	Woodchip	Sucrose	Experiment1	Blank
0.1543	0.2762	0.0068	0.0453	0.007	0.1569	0
0.1542	0.2749	0.0069	0.0446	0.0069	0.1567	0

Test 3 Equivalent sucrose concentration (mg)

Oyster	Shiitake	Char	Woodchip	Sucrose	Experiment1	Blank
1.388	2.484	0.061	0.407	0.06	1.41	0
1.387	2.472	0.062	0.401	0.06	1.41	0

A.2 Moisture Calibration Curve

On 25 June 2024, a soil calibration method was employed to measure the moisture content in a fungus sample. The process involved initially calibrating the soil moisture, followed by the calibration of biochar and woodchip. This was necessary because the fungus was grown using biochar and woodchips instead of soil. The calibration of biochar and woodchip moisture content was carried out on 4 July 2024. Subsequently, a final test was conducted to create a calibration curve accounting for all the mixed elements, including soil, biochar, and woodchip, to ensure accurate measurement of moisture content in the fungus sample.

A.2.1 Soil Moisture Calibration

Soil Moisture Readings

Table A-5 Soil moisture data

soil (gm)	Water (gm)	Total Weight Before Heating (gm)	Total Weight After Heating (gm)	Moisture	Initial Arduino Readings (1000)	Arduino Readings After 24 hr in room temperature
20	0	20	20.2	0.00	5	3
20	2	22	21.3	0.09	15	7
20	3	23	21.5	0.13	50	12
20	5	25	23.8	0.20	85	44
20	6	26	25	0.23	129	100
20	8	28	26.8	0.29	202	133
20	0	20	19.5	0.00	2	0
20	10	30	19.1	0.33	490	1
20	20	40	19	0.50	568	3
20	30	50	19.9	0.60	580	5
20	40	60	19.8	0.67	611	2
20	50	70	19.7	0.71	640	2
20	60	80	20.4	0.75	708	3

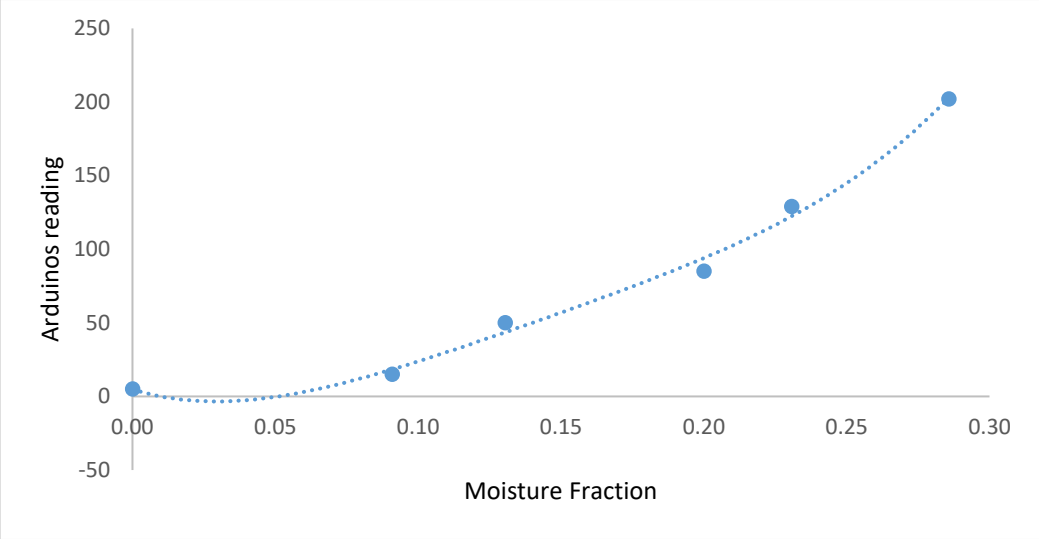

Figure A-1 Soil Moisture calibration curve

A.2.2 Biochar Moisture Calibration

Table A-6 Biochar moisture calibration

Biochar (gm)	Woodchip(gm)	Water (gm)	Total Weight before Heating (gm	Total Weight After Heating(gm)	Moisture	Initial Arduino Readings (1000)	Arduino Readings After 24hr in room temperature
20	5	0	25	25	0.00	58	50
20	5	2	27	26.5	0.07	158	151
20	5	3	28	27	0.11	114	102
20	5	5	30	28.8	0.17	386	295
20	5	6	31	30.5	0.19	456	162
20	5	8	33	31.2	0.24	555	200
20	5	10	35	34.1	0.29	567	243
20	5	0	25	22	0.00	3	0
20	5	10	35	23.1	0.29	767	4

20	5	20	45	22.5	0.44	805	3
20	5	30	55	22.9	0.55	762	2
20	5	40	65	22.1	0.62	674	1
20	5	50	75	22.5	0.67	737	2
20	5	60	85	18.4	0.71	757	3

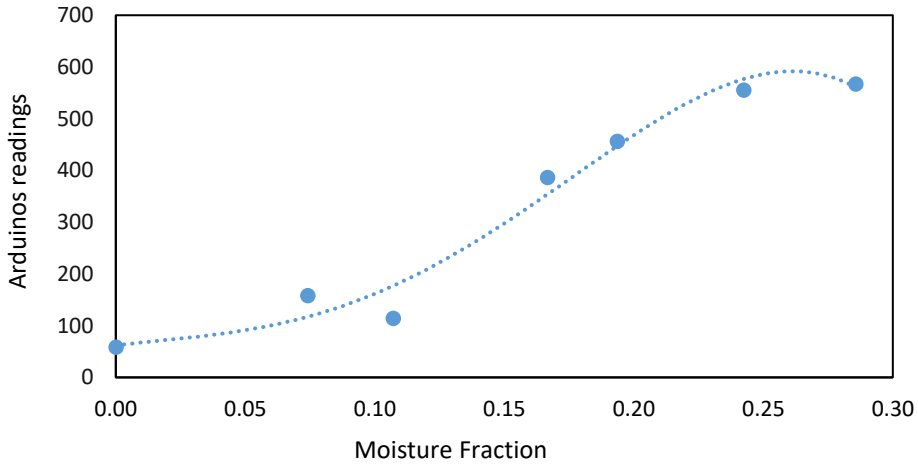

Figure A-2 Biochar Moisture calibration curve

The purpose of calibrating the moisture in soil and biochar is to assess the moisture content in the biochar. Biochar is the key material in this experiment because it serves as the growth medium for three types of mushrooms—shiitake, oyster, and pekepeke—and is also used for PFAS adsorption. The moisture calibration helps determine how much water the biochar can absorb before and after heating. Arduino sensors are used to measure the moisture content, with the readings increasing significantly between 0.10 and 0.25 moisture fractions.

A.2.3 Moisture Calibration of Soil, Biochar, and Woodchip mixture

Moisture readings of Soil, Biochar, and woodchip mixture

Table A-7 Soil, Biochar and woodchip moisture data

Soil	Char	Woodchip	Water	Total weight	Initial Arduinos Readings	Moisture
20	20	5	10	55	270	0.18
20	20	5	20	65	553	0.31
20	20	5	30	75	620	0.4
20	20	5	40	85	687	0.47
20	20	5	50	95	711	0.53

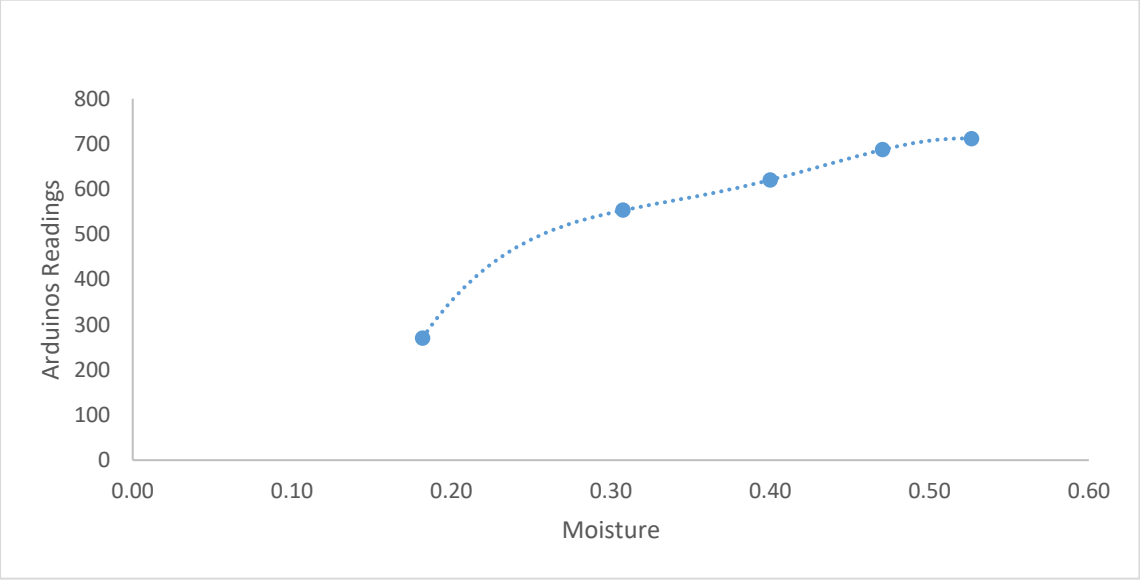

Figure A-3 Soil, Biochar, and woodchip moisture calibratio

A.3 Fungal Moisture Content

A.3.1 Experiment 7: Moisture Content Calibration

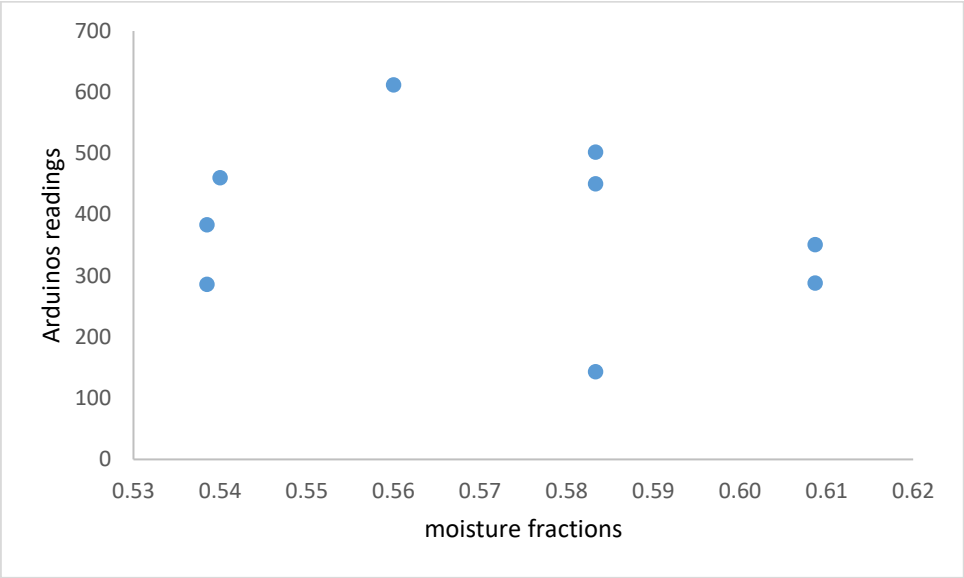

Figure A-4 Calibration curve of exp 7

A.3.2 Experiment 6: Moisture Content Calibration

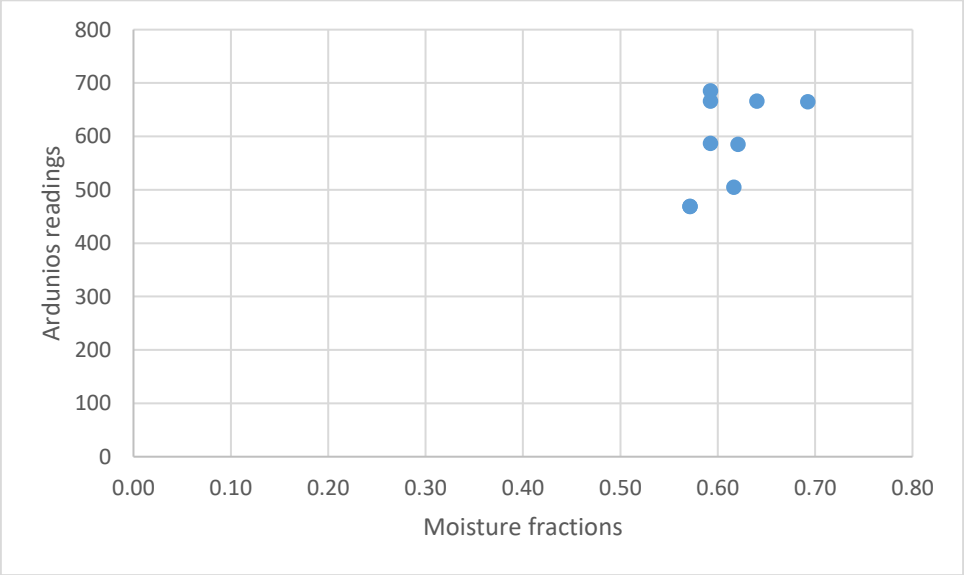

Figure A-5 Calibration curve of exp 6

A.3.3 Experiment 3: Moisture Content Calibration

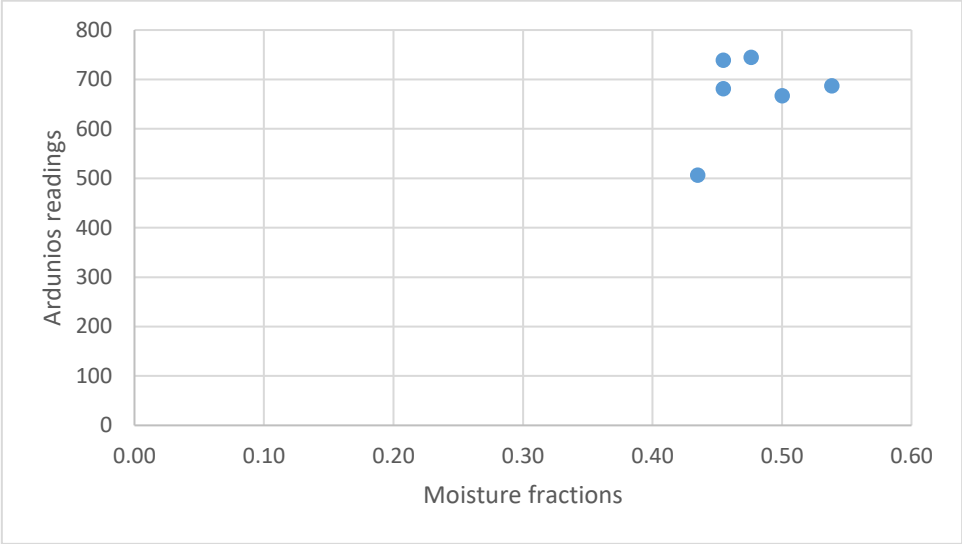

Figure A-6 Calibration curve of exp 3

A.4: Chloroform Fumigation trial test

Table A-8 Fumigation test

Test 1						
Oyster	Shiitake	Char	Woodchip	Sucrose	Experiment 1	Blank
0.1436	0.1461			0.0531		0.0078
0.1435	0.1485			0.0434		0.0089

Test 2						
Oyster	Shiitake	Char	Woodchip	Sucrose	Experiment1	Blank
0.1762	0.2981	0.0287	0.0672	0.0289	0.1788	0.0219
0.1765	0.2972	0.0292	0.0669	0.0292	0.179	0.0223

Test 3						
Oyster	Shiitake	Char	Woodchip	Sucrose	Experiment1	Blank

0.0451	0.1059	-0.0207	-0.0041	-0.0176	0.063	0.5453
0.0449	0.1032	-0.0205	-0.0034	-0.0178	0.0639	0.545

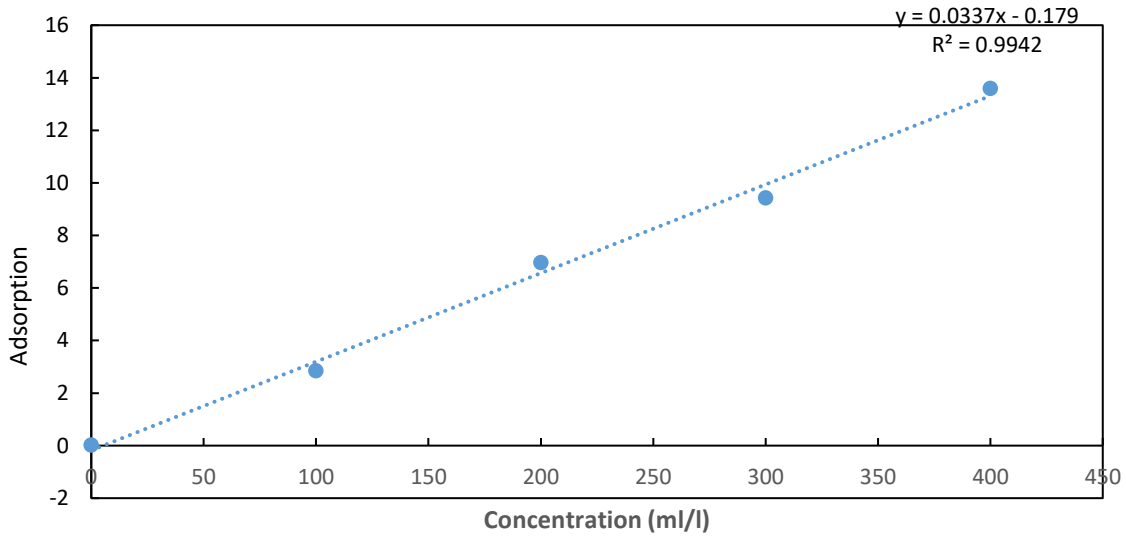

Figure A-7 Calibration curve of highly concentrated humic acid

These two Figures illustrate the adsorption of humic acid onto biochar. The humic acid concentration ranges from 0 to 30 g/L, with adsorption levels between 0.0 and 0.9 AU. Due to the high humic acid concentration in the samples, the biochar demonstrated a strong ability to adsorb the humic acid. As the concentration of humic acid increases, the adsorption also rises, reflecting highly efficient adsorption behavior within this concentration range. Therefore, the biochar effectively adsorbed this amount of humic acid.